AD-A160 971 ON THE SECONDARY BIFURCATION OF THREE DIMENSIONAL STANDING WAVES(U) WISCONSIN UNIV-MADISON MATHEMATICS RESEARCH CENTER T J BRIDGES JUL 85 MRC-TSR-2839 1/1

UNCLASSIFIED DAAG29 -80-C-0041 F/G 12/1 NL

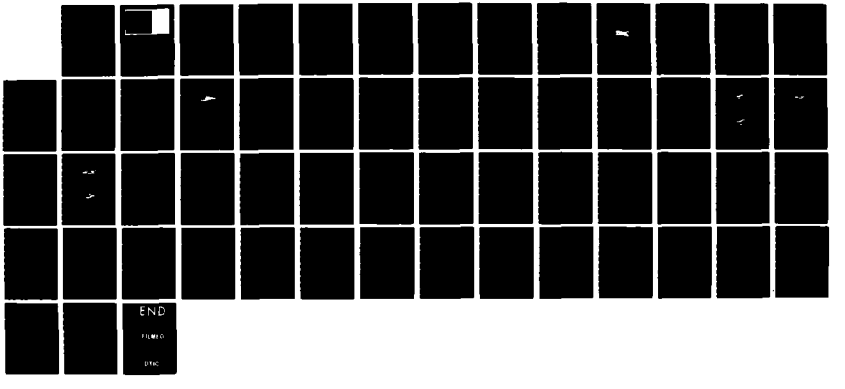

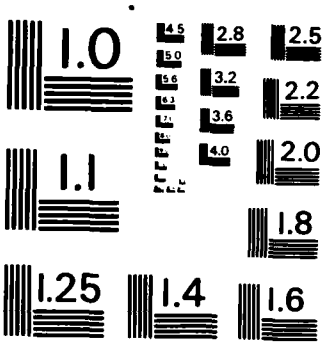

MRC Technical Summary Report #2839

ON THE SECONDARY BIFURCATION OF THREE DIMENSIONAL STANDING WAVES

Thomas J. Bridges

MIPAC Facility Document No. 3

Mathematics Research Center
University of Wisconsin—Madison
610 Walnut Street
Madison, Wisconsin 53705

July 1985

(Received May 29, 1985)

Sponsored by

U. S. Army Research Office
P. O. Box 12211
Research Triangle Park
North Carolina 27709

National Science Foundation
Washington, D. C. 20550

UNIVERSITY OF WISCONSIN-MADISON
MATHEMATICS RESEARCH CENTER

ON THE SECONDARY BIFURCATION OF THREE DIMENSIONAL STANDING WAVES

Thomas J. Bridges
Technical Summary Report #2839

July 1985

ABSTRACT

This paper contains an analysis of the complex set of periodic solutions which may occur in a fluid filled vessel of rectangular cross section. A previous analysis by Verma and Keller [2] found only simple eigenvalues for the linearized problem. It is shown herein that at critical values of the vessel aspect ratio double eigenvalues occur. Eight non-linear solution branches are emitted from these double eigenvalues. The solutions along the various branches are derived, and the results displayed graphically. It is shown that irregular waves occur along some of these branches.

In an interesting development, Bauer, Keller, and Reiss [4], in their analysis of shell buckling, showed that the splitting of multiple eigenvalues may lead to secondary bifurcation. This theory is applied to the non-linear standing wave problem herein, and it is shown that secondary bifurcation does occur in the neighborhood of the double eigenvalue. A perturbation method is used to find the secondary bifurcation points, and the solutions along the secondary branches, in the neighborhood of their respective branch points, are found.

The neighborhood around the critical aspect ratios is substantial, suggesting that secondary branching may occur in a variety of vessels with rectangular cross section. This theory offers an explanation of the irregular waves often observed in the "sloshing" of fluid in a rectangular vessel.

AMS (MOS) Subject Classifications: 76B15, 35B10, 35B32, 35R35

Key Words: Three-Dimensional Non-Linear Standing Waves, Multiple eigenvalues, secondary bifurcation

Work Unit Number 2 - Physical Mathematics

Sponsored by the United States Army under Contract No. DAAG29-80-C-0041. This material is based upon work supported by the National Science Foundation under Grant No. DMS-8210950, Mod.1.

SIGNIFICANCE AND EXPLANATION

This paper contains an analysis of the complex set of periodic solutions which may occur in a fluid filled vessel of rectangular cross section. A previous analysis by Verma and Keller [2] found only simple eigenvalues for the linearized problem. It is shown herein that at critical values of the vessel aspect ratio double eigenvalues occur. Eight non-linear solution branches are emitted from these double eigenvalues. The solutions along the various branches are derived, and the results displayed grapahically. It is shown that irregular waves occur along some of these branches.

In an interesting development, Bauer, Keller, and Reiss [4], in their analysis of shell buckling, showed that the splitting of multiple eigenvalues may lead to secondary bifurcation. This theory is applied to the non-linear standing wave problem herein, and it is shown that secondary bifurcation does occur in the neighborhood of the double eigenvalue. A perturbation method is used to find the secondary bifurcation points, and the solutions along the secondary branches, in the neighborhood of their respective branch points, are found.

The neighborhood around the critical aspect ratios is substantial, suggesting that secondary branching may occur in a variety of vessels with rectangular cross section. This theory offers an explanation of the irregular waves often observed in the "sloshing" of fluid in a rectangular vessel.

ON THE SECONDARY BIFURCATION OF THREE DIMENSIONAL STANDING WAVES

Thomas J. Bridges

1. Introduction

In a rectangular basin with vertical sides, it is well known that, if the amplitude is very small, the wave field in the basin will be a set of elementary cosine waves in the two horizontal dimensions with a particular natural frequency, which is merely a function of the basin geometry and gravity (viscosity, and surface tension, etc., being neglected). This is the classical linear standing wave solution [1, Lamb, p. 364]. As the amplitude of the wave field is increased, the number of solutions and their type is increased dramatically.

Considering a cuboidal container, the relevant parameters are the dimensionless depth, δ, and the aspect ratio, ξ, of the horizontal cross section. As the amplitude of the wave field is increased, these two parameters govern the type and multiplicity of solutions which arise. However, there is two distinct types of secondary branching which take place in this problem. One is due to the parameter δ and is only weakly dependent on ξ (*in fact, this bifurcation involves branching away from standing waves to other types of waves (sometimes travelling waves)*), and the other is due to the parameter ξ and is only weakly dependent on δ. In both cases the other parameter affects the secondary bifurcation, and the interaction can be complex, but the two phenomena remain when the other parameter is excluded. This enables the two secondary bifurcations to be isolated and studied individually. The bifurcation which is due to δ and remains when the flow-field is two-dimensional will be considered in a separate study. The purpose of this paper is to study the multiple and secondary bifurcations which arise due to the

Sponsored by the United States Army under Contract No. DAAG29-80-C-0041. This material is based upon work supported by the National Science Foundation under Grant No. DMS-8210950, Mod. 1.

effect of ξ, the basin aspect ratio. A rectangular vessel with vertical sides and infinite depth is adopted to illustrate this phenomena.

The lowest natural frequency, of such a basin, and the solutions in the neighborhood of this point have been found by Verma and Keller [2]. These solutions were found using a perturbation procedure in the amplitude, ε, and they determined the effect on the natural frequency, of the amplitude, to $O(\varepsilon^3)$. However, by concentrating on a single mode, this analysis missed the complex interactions which may take place between some modes and the secondary bifurcation which also occurs on some primary branches. In Section 2, an analysis, similar to Verma and Keller, is used to determine the complete set of primary bifurcation points and the solutions along the simple primary branches. This analysis shows that each of the primary bifurcation points occurs at $\sigma_0 = \lambda_{m,n}^{1/2}$, where

$$\lambda_{m,n} = \pi(m^2 + \xi^2 n^2)^{1/2} \tag{1.1}$$

where m and n are the mode numbers, respectively, in the x- and z-directions. For particular combinations of ξ, m and n, multiple eigenvalues, of multiplicity two, will occur. For example, if $\xi = 1$ (a square basin), every pair (m,n), $m \neq n$ is a double eigenvalue. If $\xi = 1/2$, then $\lambda_{1,4} = \lambda_{2,2}$, etc. In fact, for ξ equal to any rational fraction there is a set of double eigenvalues. The physical reason for the appearance of double eigenvalues is quite obvious. In a square vessel, for example, the linear sinusoidal wave field with 2-wavelengths in the x-direction and 1-wavelength in the z-direction will share the same natural frequency with a wave form which has 1-wavelength in the x-direction and 2 wavelengths in the z-direction. Therefore, although the eigenvalue is double, the eigenfunctions are linearly independent. This is, in fact, a ramification of spatial symmetry, a subject which is discussed in a more general context by Sattinger [3].

In Section 3, an analysis of these double primary bifurcation points is performed. It is found that from each of these points there extends 8 branches (4 of these branches correspond to $-\varepsilon$, and are reflections of the $+\varepsilon$ branches). Of the four $+\varepsilon$ branches

two correspond to the two linearly independent eigenfunctions taken separately, and the other two correspond to mixed modes involving both of the eigenfunctions. These mixed modes combine to produce irregular surface wave fields which for some cases appear to be spatially random to the uninitiated observer. Figures depicting solutions of this type are given in Section 3.

In an intersting discovery, Bauer, Keller, and Reiss [4] observed that as a multiple bifurcation point is "split" (by varying an auxiliary parameter (in this case ξ)) into primary bifurcation points a secondary bifurcation may occur. At the double eigenvalue, which arises in the standing wave problem, there are four $+\varepsilon$ branches. Upon splitting this point, two of these branches become the simple primary branches. Due to continuous dependence, the other two solutions cannot simply vanish when ξ is perturbed away from ξ_0, the location of the double eigenvalue, and therefore they slowly depart by creeping up the split primary branches in a manner which differs from problem to problem. Bauer, Keller, and Reiss developed a perturbation method which enabled them to analyze this phenomena in the buckling of thin shells. Subsequently, this theory has been successfully applied by Mahar and Matkowsky [5] to a model biochemical reaction problem, Matkowsky, Putnick, and Reiss [6] to the buckling of rectangular plates, and has been extended to the bifurcation from triple eigenvalues, which results in secondary and tertiary bifurcation, by Reiss [7].

In Section 4 the theory of Bauer, Keller, and Reiss is used to show that secondary bifurcation occurs in the neighborhood of the double points which arise in the problem of three-dimensional standing waves. The secondary bifurcation points are found and the solutions along them are derived. It is found that mode jumping occurs in the shift from the primary to the secondary branches and the complex interaction of the two modes in the neighborhood of the secondary bifurcation point produces irregular wave forms.

These mixed-mode solutions offer an explanation of some of the irregularities that are often observed in experiments. For example, in the experiments of Taylor [8], on the highest two dimensional standing waves, irregular three-dimensional "crown waves" were

observed forming on top of the two-dimensional standing waves. His experimental basin had an aspect ratio of $\xi \sim 2.0$, and the crown waves look like mixed-mode solutions discussed herein.

2. Primary Bifurcation from Simple Eigenvalues

The fluid in the basin is taken to be inviscid, irrotational, and absent of surface tension. The problem can then be expressed in terms of a potential function and the wave height. Length scales are rendered dimensionless by 2a, the tank length (see Figure 1), with the exception of the z-direction where 2b, the tank width is used, and g, the acceleration of gravity, and the frequency arc used for the time scales. The governing equations and boundary conditions are

$$\frac{\partial^2 \phi^*}{\partial x^2} + \frac{\partial^2 \phi^*}{\partial y^2} + \xi^2 \frac{\partial^2 \phi^*}{\partial z^2} = 0$$

$$\text{for } -1/2 \leq x \leq 1/2, \; -\frac{1}{2} \leq z \leq \frac{1}{2}, \; -\infty < y \leq \eta^*(x,z,t) \tag{2.1}$$

$$\frac{\partial \phi^*}{\partial x} = 0 \quad \text{at} \quad x = \pm 1/2 \tag{2.2a}$$

$$\frac{\partial \phi^*}{\partial z} = 0 \quad \text{at} \quad z = \pm 1/2 \tag{2.2b}$$

$$\frac{\partial \phi^*}{\partial y} \to 0 \quad \text{as} \quad y \to -\infty \tag{2.2c}$$

$$\omega^* \frac{\partial \phi^*}{\partial t} + \frac{1}{2}\left[(\phi_x^*)^2 + (\phi_y^*)^2 + \xi^2(\phi_z^*)^2\right] + \eta^* = 0 \quad \text{on} \quad y = \eta^* \tag{2.3}$$

$$\omega^* \frac{\partial \eta^*}{\partial t} + \phi_x^* \frac{\partial \eta^*}{\partial x} + \xi^2 \phi_z^* \frac{\partial \eta^*}{\partial z} - \frac{\partial \phi^*}{\partial y} = 0 \quad \text{on} \quad y = \eta^* \tag{2.4}$$

$\phi^* = \eta^* = 0$ is a solution for all values of ξ. This is the basic state. Periodic solutions, of period ω^*, which bifurcate from this state are sought. The potential function and the wave height are assumed to have an expansion of the following form,

$$\phi^*(x,y,z,t;\xi;\varepsilon) = \varepsilon\phi_1(x,y,z,t;\xi) + \varepsilon^2\phi_2(x,y,z,t;\xi) + \ldots \tag{2.5a}$$

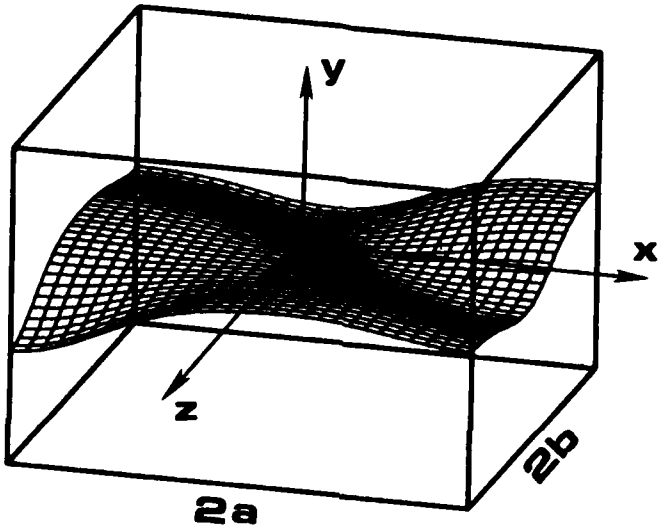

Figure 1. Definitional figure showing coordinate system and vessel geometry.

$$\eta^*(x,z,t;\xi;\varepsilon) = \varepsilon\eta_1(x,z,t;\xi) + \varepsilon^2\eta_2(x,z,t;\xi) + \ldots \tag{2.5b}$$

$$\omega^*(\xi;\varepsilon) = \sigma_0(\xi) + \varepsilon\sigma_1(\xi) + \varepsilon^2\sigma_2(\xi) + \ldots \tag{2.5c}$$

and ε, a measure of the wave amplitude, is chosen to be proportional to the first term in (2.5b). Before substitution of (2.5) into the boundary value problem, the free surface boundary conditions (2.3) and (2.4) are expanded in a Taylor series about $y = 0$,

$$F(x,y,z,t;\xi;\varepsilon)\Big|_{y=\eta^*} = F\Big|_{y=0} + \frac{\partial F}{\partial y}\Big|_{y=0}\eta^* + \frac{1}{2}\frac{\partial^2 F}{\partial y^2}\Big|_{y=0}\eta^{*2} + \ldots \tag{2.6}$$

Substitution of (2.5) into (2.1) - (2.4), the use of (2.6), and the setting to zero of the terms proportional to each power of ε results in the following sequence of boundary value problems,

$$\frac{\partial^2\phi_j}{\partial x^2} + \frac{\partial^2\phi_j}{\partial y^2} + \xi^2\frac{\partial^2\phi_j}{\partial z^2} = 0$$

$$\text{in } -\tfrac{1}{2} < x < \tfrac{1}{2}, \quad -\tfrac{1}{2} < z < \tfrac{1}{2}, \quad -\infty < y < 0 \tag{2.7}$$

$$\frac{\partial\phi_j}{\partial x} = 0 \quad \text{at} \quad x = \pm\tfrac{1}{2} \tag{2.8a}$$

$$\frac{\partial\phi_j}{\partial z} = 0 \quad \text{at} \quad z = \pm\tfrac{1}{2} \tag{2.8b}$$

$$\frac{\partial\phi_j}{\partial y} \to 0 \quad \text{as} \quad y \to -\infty \tag{2.8c}$$

$$\sigma_0\frac{\partial\phi_j}{\partial t} + \eta_j = R_j \quad \text{at} \quad y = 0 \tag{2.9}$$

$$\sigma_0\frac{\partial\eta_j}{\partial t} - \frac{\partial\phi_j}{\partial y} = S_j \quad \text{at} \quad y = 0 \tag{2.10}$$

for $j = 1, 2, \ldots$. $R_1 = S_1 = 0$, and R_j and S_j for $j > 1$ are functions of terms of previous order only, and are given in Appendix I. Since (2.7) - (2.10) for $j > 1$ are inhomogeneous eigenvalue problems, they are soluable if and only if they satisfy the Fredholm alternative. The alternative necessary for this and the later developments is given in Appendix II.

The solution of (2.7) - (2.10) for $j = 1$ is

$$\eta_1 = \cos \alpha_m \bar{x} \cos \beta_n \bar{z} \sin t \tag{2.11}$$

$$\phi_1 = \sigma_0^{-1} e^{\lambda_{m,n} y} \cos \alpha_m \bar{x} \cos \beta_n \bar{z} \cos t \tag{2.12}$$

where $\alpha_m = m\pi$, $\beta_n = n\pi$, $\bar{x} = x + \frac{1}{2}$, $\bar{z} = z + \frac{1}{2}$, and

$$\sigma_0^2 = \lambda_{m,n} = (\alpha_m^2 + \xi^2 \beta_n^2)^{\frac{1}{2}} \tag{2.13}$$

At the next order, the solvability condition requires that $\sigma_1 = 0$, then

$$\begin{aligned} \eta_2 = {} & (B_{21} + C_{21} \cos 2t) \cos 2\alpha_m \bar{x} \\ & + (B_{22} + C_{22} \cos 2t) \cos 2\beta_n \bar{z} \\ & + (B_{23} + C_{23} \cos 2t) \cos 2\alpha_m \bar{x} \cos 2\beta_n \bar{z} \end{aligned} \tag{2.14}$$

and

$$\phi_2 = [A_{20} + A_{21} e^{2\alpha_m y} \cos 2\alpha_m \bar{x} + A_{22} e^{2\xi\beta_n y} \cos 2\beta_n \bar{z}] \sin 2t \tag{2.15}$$

where

$$A_{20} = -\sigma_0/8 \tag{2.16a}$$

$$A_{21} = \frac{\xi^2 \beta_n^2}{4\sigma_0(\alpha_m - 2\sigma_0^2)} \tag{2.16b}$$

$$A_{22} = \frac{\alpha_m^2}{4\sigma_0(\xi\beta_n - 2\sigma_0^2)} \tag{2.16c}$$

$$B_{21} = \frac{\alpha_m^2}{8\sigma_0^2} \tag{2.17a}$$

$$B_{22} = \frac{\xi^2 \beta_n}{8\sigma_0^2} \tag{2.17b}$$

$$B_{23} = \sigma_0^2/8 \tag{2.17c}$$

$$C_{21} = -2\sigma_0 A_{21} - \frac{(\sigma_0^4 + \xi^2\beta_n^2)}{8\sigma_0^2} \tag{2.17d}$$

$$C_{22} = -2\sigma_0 A_{22} - \frac{(\sigma_0^4 + \alpha_m^2)}{8\sigma_0^2} \tag{2.17e}$$

$$C_{23} = -\sigma_0^2/8 \tag{2.17f}$$

After some manipulation, the solvability condition at the next order results in an expression for σ_2, the amplitude correction to the natural frequency,

$$\sigma_2 = -\frac{\sigma_0^5}{8} - \frac{3(\alpha_m^4 + \xi^4\beta_n^4)}{32\sigma_0^3} + \frac{\xi^4\beta_n^4}{4\sigma_0(2\sigma_0^2 - \alpha_m)} + \frac{\alpha_m^4}{4\sigma_0(2\sigma_0^2 - \xi\beta_n)} \tag{2.18}$$

By choosing $\alpha_m = \beta_n = 1$ and $\xi = 1/L$, this result is in agreement with that found by Verma and Keller for the first mode when the depth is infinite. The expression (2.18) is negative definite and this can be shown by recasting (2.18) as

$$\sigma_2 = \sigma_0\left[\frac{-4\sigma_0^{10} + 2\xi\beta_n\sigma_0^8 + 2\alpha_m^4\sigma_0^2 + 3\xi\beta_n\alpha_m^4}{32\sigma_0^4(2\sigma_0^2 - \xi\beta_n)}\right]$$

$$+ \sigma_0\left[\frac{-4\sigma_0^{10} + 2\alpha_m\sigma_0^8 + 2\xi^4\beta_n^4\sigma_0^2 + 3\alpha_m\xi^4\beta_n^4}{32\sigma_0^4(2\sigma_0^2 - \alpha_m)}\right] \tag{2.19}$$

With no loss of generality, choose $\xi\beta_n = r\alpha_m$ where $r \in [0,\infty]$. Then (2.19) can be expressed as

$$\frac{32\sigma_2}{\alpha_m^2\sigma_0} = \frac{\left[2\sqrt{1+r^2}(1 - 2(1+r^2)^2) + r(3 + 2(1+r^2)^2)\right]}{(1+r^2)(2\sqrt{1+r^2} - r)}$$

$$+ \frac{\left[2\sqrt{1+r^2}(r^4 - 2(1+r^2)^2) + (3r^4 + 2(1+r^2)^2\right]}{(1+r^2)(2\sqrt{1+r^2} - 1)} \tag{2.19a}$$

For subcritical bifurcation it is required that

$$2\sqrt{1 + r^2}(1 - 2(1 + r^2)^2) + r(3 + 2(1 + r^2)^2) < 0 \tag{2.20a}$$

and

$$2\sqrt{1 + r^2}(r^4 - 2(1 + r^2)^2) + (3r^4 + 2(1 + r^2)^2) < 0 \tag{2.20b}$$

for any $r \in [0,\infty]$. After some algebraic manipulation (2.20a) can be recast as

$$-\left[4 + 3r^2 + 40r^4 + 92r^6 + 64r^8 + 12r^{10}\right] < 0 \tag{2.21a}$$

and (2.20b) can be recast as

$$-\left[2 + 12p + 8p^2 + 4p^3 + 5p^4 + 2p^5\right] < 0 \tag{2.21b}$$

where $p = \sqrt{1 + r^2} - 1$, which satisfies $p \in [0,\infty]$ when $r \in [0,\infty)$. The pair (2.21a,b) proves the conjecture: the bifurcation from all the simple eigenvalues is subcritical. The natural frequency of the standing wave decreases as the amplitude increases. There is also the interesting feature that $|\sigma_2|$ increases with increasing m and n. Therefore the magnitude of the slope in the ω^*-ε plane decreases with increasing mode number resulting in an intersection of the higher mode branches with the lower mode branches.

Figure 2 is a plot of the natural frequency as a function of amplitude for $\xi = .25$ and m, n ranging over 1, 2, and 3. The dashed lines correspond to modes with equal indices ($m = n$). This is an almost two dimensional field and the 9 modes are coalescing around the 3 two-dimensional values. In Figure 3, for the same range of m and n, and $\xi = 1.1$, the modes are plotted. Here they are more spread out with the mode intersections being quite obvious. In Figure 4, a typical non-linear wave on a branch bifurcating from a simple eigenvalue, is plotted. The vessel is square in cross-section ($\xi = 1$), $\varepsilon = 0.15$, and $m = n = 1$. This is often referred to as the "slosh" mode. Figure 5 shows a time series for the wave height in the left front corner ($\bar{x} = \bar{z} = 0$), of the tank depicted in Figure 4. Figure 4 is a "snapshot" corresponding to $\frac{t}{2\pi} = \frac{3}{4} \pm k$, $k = 0,1,2, \ldots$.

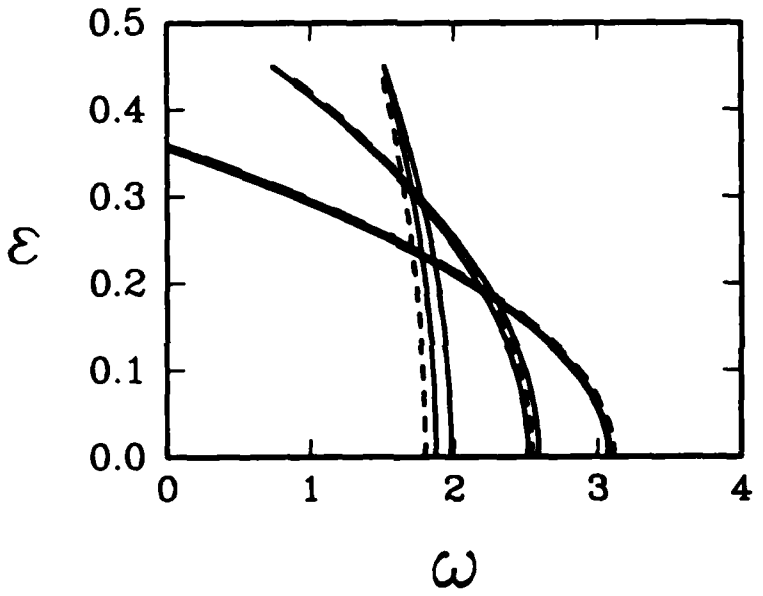

Figure 2. Bifurcation diagram for simple eigenvalues at $\xi = .25$, and mode numbers (m,n) ranging over 1, 2, and 3. The dashed lines correspond to branches with equal indices $(m = n)$.

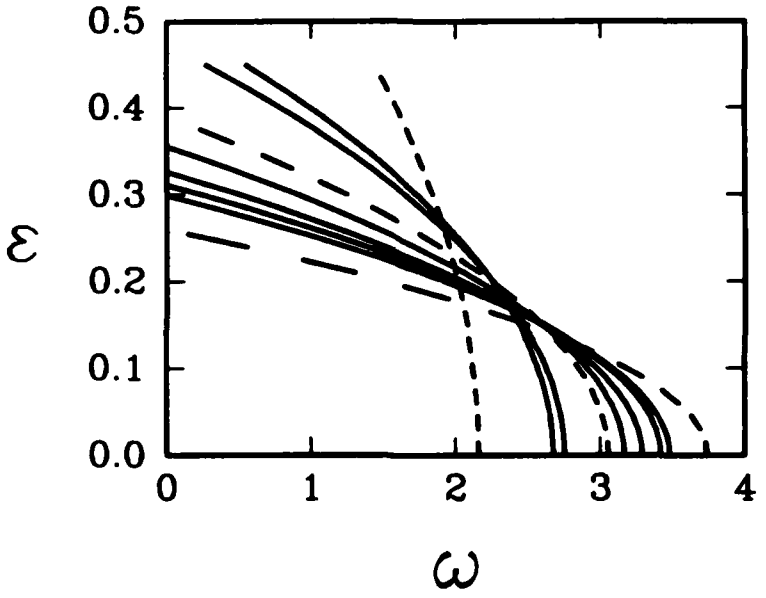

Figure 3. Bifurcation diagram for simple eigenvalues at $\xi = 1.1$, and mode numbers (m,n) ranging over 1, 2, and 3. The dashed lines correspond t› branches with equal indices (m = n).

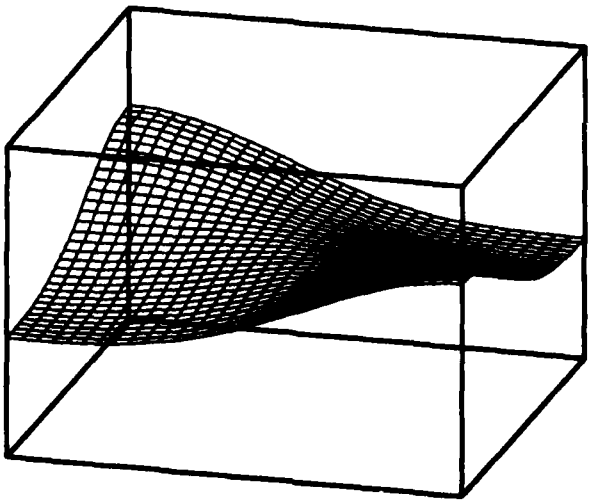

Figure 4. Spatial variation of the solution for $\xi = 1$, $m = n = 1$, and $\varepsilon = 0.15$ at a fixed time: $\frac{t}{2\pi} = \frac{3}{4} \pm k$, $k = 0, 1, 2, \ldots$. This is often referred to as the "slosh" mode.

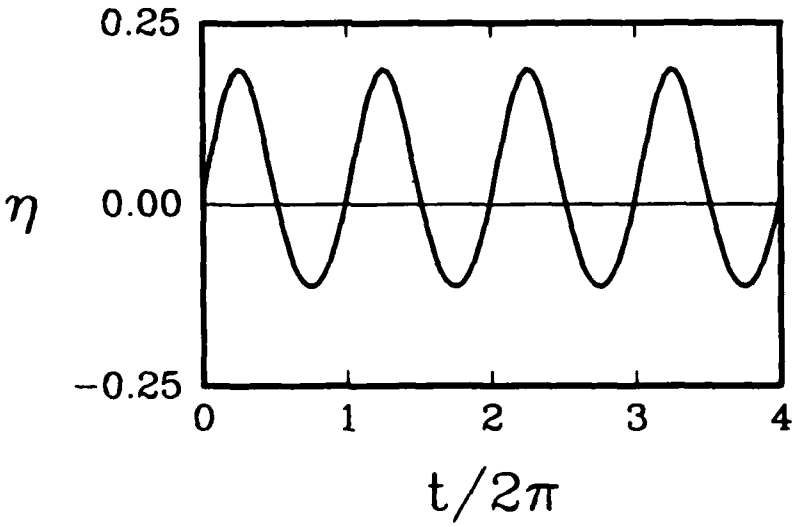

Figure 5. Time series of the wave height, in the left front corner ($\bar{x} = \bar{z} = 0$) of the vessel in Figure 4. The parameters are $\xi = 1.0$, $m = n = 1$, and $\varepsilon = 0.15$.

In summary, the primary bifurcation points are at $\sigma_0 = \sqrt{\pi}\,(m^2 + \xi^2 n^2)^{1/4}$ with $m = 1, 2, \ldots$ and $n = 1, 2, \ldots$ and the solutions on the primary branches, for values of ξ, m, and n such that the eigenvalues are simple, as $\varepsilon \to 0$, are

$$\phi^* = \varepsilon\phi_1 + \varepsilon^2\phi_2 + 0(\varepsilon^3) \tag{2.22}$$

$$\eta^* = \varepsilon\eta_1 + \varepsilon^2\eta_2 + 0(\varepsilon^3) \tag{2.23}$$

$$\omega^* = \sigma_0 + \varepsilon^2\sigma_2 + 0(\varepsilon^3) \tag{2.24}$$

3. Primary Bifurcation From the Double Eigenvalues

At critical values of the aspect ratio of the vessel cross-section, a set of double eigenvalues will occur. When $\xi = 1$ there is a double eigenvalue for any pair (m,n) such that $m \neq n$, and when $\xi = 1/2$ $(m,n) = (1,4)$ and $(m,n) = (2,2)$ is a double eigenvalue, ad infinitum. For ξ equal to any rational fraction there is a set of double eigenvalues. It is expected that the nature of the solutions will be similar for the various critical values of ξ. To elaborate this phenomena, an analysis of the solutions emitted from the set of double eigenvalues for a square vessel, $\xi = 1$, is performed. In this case the bifurcation points are given by

$$\sigma_0 = (\alpha_m^2 + \beta_n^2)^{1/4} \tag{3.1}$$

The potential function and wave height are again expanded in a perturbation series in ε,

$$\phi^*(x,y,z,t;\xi;\varepsilon) = \varepsilon\phi_1(x,y,z,t;\xi) + \varepsilon^2\phi_2(x,y,z,t;\xi) + \ldots \tag{3.2a}$$

$$\eta^*(x,z,t;\xi,\varepsilon) = \varepsilon\eta_1(x,z,t;\xi) + \varepsilon^2\eta_2(x,z,t;\xi) + \ldots \tag{3.2b}$$

$$\omega^*(\xi,\varepsilon) = \sigma_0(\xi) + \varepsilon^2\sigma_1(\xi) + \varepsilon^2\sigma_2(\xi) + \ldots \tag{3.3}$$

However, the symbols here should not be confused with those in Section 2. Outside of the obvious similarities, the results in Section 2 are distinct from the results contained herein. In fact they are the complement of each other.

Substituting (3.2) and (3.3) into the governing equations and boundary conditions (2.1) - (2.4) and equating terms proportional to like powers of ε to zero results in the sequence of boundary value problems given in (2.7) - (2.10) but with the R_j and S_j differing upon substitution.

With $R_1 = S_1 = 0$, and the fact that there is a double eigenvalue with a two-dimensional null space, the first order solution is

$$\eta_1 = [A_{11}\cos \alpha_m\bar{x} \cos \beta_n\bar{z} + A_{12}\cos \beta_n\bar{x} \cos \alpha_m\bar{z}] \sin t \tag{3.4}$$

and

$$\phi_1 = \sigma_0^{-1}[A_{11}\cos\ \alpha_m\bar{x}\ \cos\ \beta_n\bar{z} + A_{12}\cos\ \beta_n\bar{x}\ \cos\ \alpha_m\bar{z}]\ \cos\ t \tag{3.5}$$

where σ_0 is given by (3.1) and ε is chosen to be proportional to the first order wave height. This results in a relationship between A_{11} and A_{12},

$$A_{11}^2 + A_{12}^2 = 1 \tag{3.6}$$

The relative magnitudes of A_{11} and A_{12} are, however, undertermined at this order.

The problems for $j > 1$ are inhomogeneous eigenvalue problems and must satisfy the solvability condition given in Appendix II. As the nullspace at the eigenvalue is of dimension two, there will be two solvability conditions at each order. Substituting ϕ_1, η_1, etc. into R_2 and S_2, and applying the solvability condition results in $\sigma_1 = 0$, and

$$\begin{aligned}
\eta_2(x,z,t) = {} & (B_{21} + C_{21}\cos\ 2t)\ \cos\ 2\alpha_m\bar{x} \\
& + (B_{22} + C_{22}\cos\ 2t)\ \cos\ 2\alpha_m\bar{z} \\
& + (B_{23} + C_{23}\cos\ 2t)\ \cos\ 2\beta_n\bar{x} \\
& + (B_{24} + C_{24}\cos\ 2t)\ \cos\ 2\beta_n\bar{z} \\
& + (B_{25} + C_{25}\cos\ 2t)\ \cos\ (\alpha_m + \beta_n)\bar{x}\ \cos\ (\alpha_n + \beta_n)\bar{z} \\
& + (B_{26} + C_{26}\cos\ 2t)[\cos(\alpha_m + \beta_n)\bar{x}\ \cos(\alpha_m - \beta_n)\bar{z} + \\
& \qquad \cos(\alpha_m - \beta_n)\bar{x}\ \cos(\alpha_m + \beta_n)\bar{z}] \\
& + (B_{27} + C_{27}\ \cos\ 2t)\ \cos(\alpha_m - \beta_n)\bar{x}\ \cos(\alpha_m - \beta_n)\bar{z} \\
& + (B_{28} + C_{28}\ \cos\ 2t)\ \cos\ 2\alpha_m\bar{x}\ \cos\ 2\beta_n\bar{z} \\
& + (B_{29} + C_{29}\ \cos\ 2t)\ \cos\ 2\beta_n\bar{x}\ \cos\ 2\alpha_n\bar{x}
\end{aligned} \tag{3.7}$$

and

$$\begin{aligned}
\phi_2(x,y,z,t) = {} & [A_{20} + A_{21}\cos\ 2\alpha_m\bar{x}\ \exp\ (2\alpha_m y) \\
& + A_{22}\ \cos\ 2\alpha_m\bar{z}\ \exp\ (2\alpha_m y) \\
& + A_{23}\cos\ 2\bar{\beta}_n\bar{x}\ \exp\ (2\beta_n y)
\end{aligned}$$

$$+ A_{24}\cos 2\beta_n \bar{z} \exp(2\beta_n y)$$

$$+ A_{25}\cos(\alpha_m + \beta_n)\bar{x} \cos(\alpha_m + \beta_n)\bar{z} \exp[\sqrt{2}(\alpha_m + \beta_n)y]$$

$$A_{26}[\cos(\alpha_m + \beta_n)\bar{x} \cos(\alpha_m - \beta_n)\bar{z} +$$

$$+ \cos(\alpha_m - \beta_n)\bar{x} \cos(\alpha_m + \beta_n)\bar{z}]\exp[\sqrt{2}\sigma_0^2 y]$$

$$+ A_{27}\cos(\alpha_m - \beta_n)\bar{x} \cos(\alpha_m - \beta_n)\bar{z} \exp[\sqrt{2}|\alpha_m - \beta_n|y]]\sin 2t \qquad (3.8)$$

The coefficients A_{2j}, B_{2j}, and C_{2j} are given in Appendix III.

The most obvious effect of the double eigenvalue is the explosion of higher harmonics at the second order. This is to be contrasted with the solutions at simple eigenvalues where simple harmonics appear at higher order and only weakly affect the linear solution. In the case of the double eigenvalue the mixed mode solutions also result in an increasing complexity in the spatial structure, on a finer and finer scale, as the amplitude is increased.

Substituting the known terms into R_3 and S_3 and applying the two solvability conditions results in the bifurcation equations,

$$[a_1 A_{11}^2 + a_2 A_{12}^2 + 2\sigma_2] A_{11} = 0 \qquad (3.9)$$

$$[a_2 A_{11}^2 + a_1 A_{12}^2 + 2\sigma_2] A_{12} = 0 \qquad (3.10)$$

which, along with the normalization

$$A_{11}^2 + A_{12}^2 = 1 \qquad (3.11)$$

form a set of three equations for the three unknowns A_{11}, A_{12}, and σ_2. The coefficients a_1 and a_2 are given by

$$a_1 = \frac{\sigma_0^5}{4} + \frac{3(\alpha_m^4 + \beta_n^4)}{16\sigma_0^3} - \frac{\alpha_m^4}{2\sigma_0(2\sigma_0^2 - \beta_n)} - \frac{\beta_n^4}{2\sigma_0(2\sigma_0^2 - \alpha_m)} \qquad (3.12)$$

and

$$a_2 = \left(\frac{10 - 3\sqrt{2}}{4 - \sqrt{2}}\right)\frac{\sigma_0^5}{4} - \frac{3(\alpha_m^4 + \beta_n^4)}{16\sigma_0^3} - \frac{(\alpha_m - \beta_m)^4}{4\sigma_0(4\sigma_0^2 - \sqrt{2}(\alpha_m + \beta_n))}$$

$$- \frac{(\alpha_m + \beta_n)^4}{4\sigma_0(4\sigma_0^2 - \sqrt{2}|\alpha_m - \beta_n|)} \qquad (3.13)$$

The three equations (3.9) - (3.11) has the following set of solutions

Case I: $A_{02} = 0, \quad A_{01} = \pm 1, \quad \sigma_2 = -a_1/2$

Case II: $A_{01} = 0, \quad A_{02} = \pm 1, \quad \sigma_2 = -a_1/2$

Case III: $A_{01} = \pm\frac{1}{\sqrt{2}}, \quad A_{02} = \pm\frac{1}{\sqrt{2}}, \quad \sigma_2^M = -(a_1 + a_2)/4$

Case I and II are pure modes corresponding to the modes of the simple eigenvalues that coalesce to form the double point. They share the same natural frequency and are spatially symmetric. When the relevant parameters are substituted the amplitude correction to the natural frequency, $\sigma_2 = -\frac{1}{2}a_1$, agrees with the correction found for the simple eigenvalues (Eqn. (2.18)). In Section 2 it was found that this expression is negative definite, therefore $a_1 > 0$ for all positive integers m and n. Case III involves mixed modes. The leading terms are proportional to the sum and difference of the two eigenfunctions. The amplitude correction to the mixed mode solutions, σ_2^M, differs from the pure mode case by an amount $(a_1 - a_2)/4$. It has not been proved that this expression is negative for all parameter values, but it appears, from numerical evaluation, that this is in fact the case. It is therefore conjectured that the bifurcation of the mixed modes is always subcritical.

Figures 6 and 7 display the bifurcation from double eigenvalues for a vessel with a square cross-section. In Figure 6 the dashed lines correspond to the simple eigenvalues $\lambda_{1,1}$ and $\lambda_{2,2}$, and the solid lines are emitted by the double point $\lambda_{1,2}$. There are two pure modes corresponding to the upper branch (labelled p) and two mixed modes which

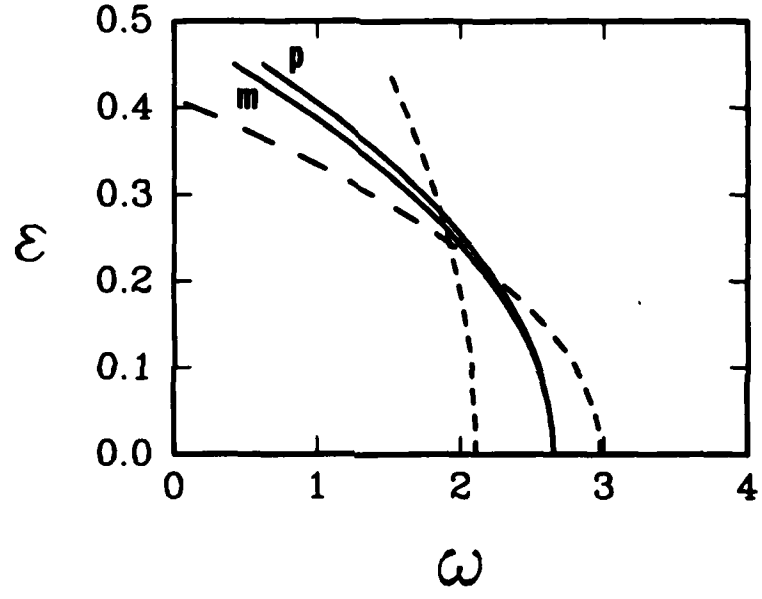

Figure 6. Bifurcation diagram of simple and double eigenvalues for $\xi = 1.0$ and m and n ranging over 1 and 2. The dashed lines correspond to the $\lambda_{1,1}$ and $\lambda_{2,2}$ branches. The upper branch emitted by the double eigen- supports two pure modes (labelled p), and the lower branch supports two mided modes (labelled m).

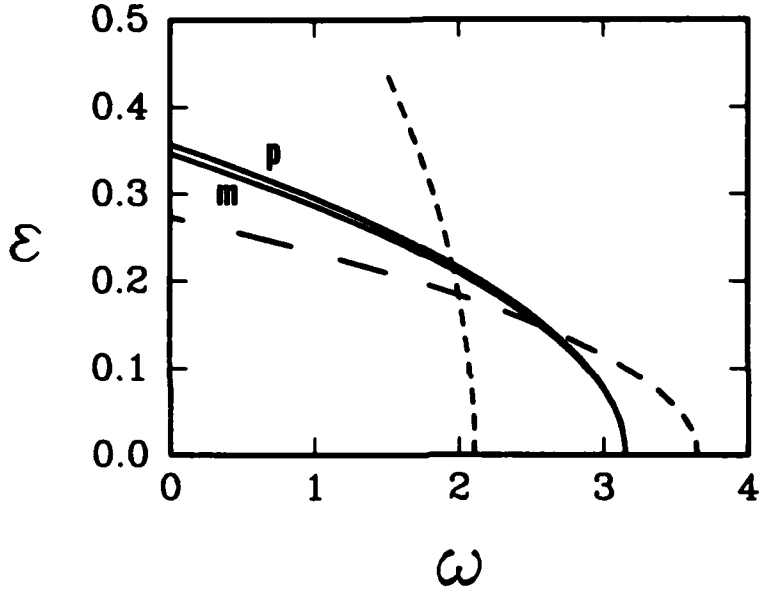

Figure 7. Bifurcation of simple and double eigenvalues for $\xi = 1.0$ and (m,n) ranging over 1 and 3. The dashed lines correspond to the $\lambda_{1,1}$ and $\lambda_{3,3}$ branches. The upper branch emitted by the double eigenvalue supports two pure modes (labelled p), and the lower branch supports two mixed modes (labelled m).

share the natural frequency on the lower branch (labelled m). Figure 7 shows a similar result with m and n ranging over 1 and 3. The dashed lines correspond to $\lambda_{1,1}$ and $\lambda_{3,3}$, and the solid lines correspond to the four branches emitted by the double point.

In Figures 8, 9, and 10 the wave fields corresponding to Figure 7 are plotted. In Figure 8, for $m = 1$, $n = 3$, and $\varepsilon = .1$, the pure mode, with $A_{11} = 1.0$ and $A_{12} = 0$ is plotted. This corresponds to the upper branch emitted from the double eigenvalue in Figure 7. In Figures 9 and 10, the results along the lower (mixed mode) branch emitted from the double eigenvalue are plotted for $\varepsilon = .1$. In Figure 9 $A_{11} = \frac{1}{\sqrt{2}}$ and $A_{12} = \frac{1}{\sqrt{2}}$, whereas in Figure 10 $A_{11} = \frac{1}{\sqrt{2}}$ and $A_{12} = -\frac{1}{\sqrt{2}}$. The mixing of the modes produces quite irregular solutions. Figures 11a, b, c show the time series for the left front corner $(\bar{x} = \bar{z} = 0)$ of the vessels depicted in Figures 8, 9, and 10. The snapshots in Figures 8, 9, and 10 correspond to the times $\frac{t}{2\pi} = \frac{3}{4} \pm k$, $k = 0,1,2, \ldots$. Figure 11a corresponds to the pure mode in Figure 8 $(A_{11} = 1, A_{12} = 0)$. Figure 11b corresponds to the mixed mode in Figure 9 $(A_{11} = 1/\sqrt{2}, A_{12} = 1/\sqrt{2})$. Figure 11c corresponds to the mixed mode in Figure 10 $(A_{11} = 1/\sqrt{2}, A_{12} = -1/\sqrt{2})$. Reference to eqn. (3.4) shows that $\eta_1 = 0$ when $\bar{x} = \bar{z} = 0$ and $A_{11} = -A_{12}$. Hence the linear effects in Figure 11c are of $0(\varepsilon^2)$ and proportional to $\cos 2t$, with the nonlinear effects coming in at $0(\varepsilon^3)$. Although the results in Figures 11a, b, and c differ markedly, all three correspond to the same set of basic parameters.

Examples for other mixed mode solutions in a square vessel are given in Figures 12 and 13. Figure 12 is of a mixed mode with $m = 2$, $n = 4$, and Figure 13 is of a mixed mode with $m = 1$, $n = 5$.

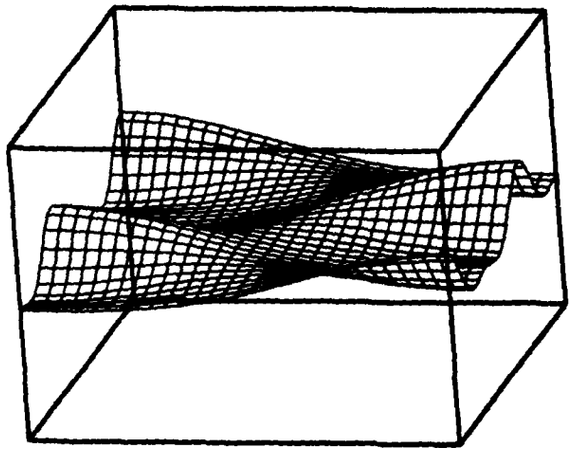

Figure 8. Spatial variation of one of the solutions along the p branch in Figure 7 at $t/2\pi = 3/4 \pm k$, $k = 0, 1, 2, \ldots$. The parameters are $\xi = 1.$, $m = 1$, $n = 3$, $\varepsilon = 0.1$, $A_{11} = 1.$, and $A_{12} = 0.$

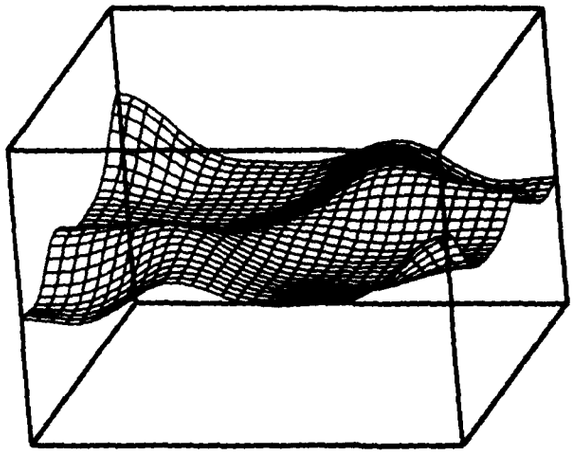

Figure 9. Spatial variation of one of the solutions along the m branch in Figure 7 at $t/2\pi = 3/4 \pm k$, $k = 0, 1, 2, \ldots$. The parameters are $\xi = 1.$, $m = 1$, $n = 3$, $\varepsilon = 0.1$, $A_{11} = 1/\sqrt{2}$, and $A_{12} = 1/\sqrt{2}$.

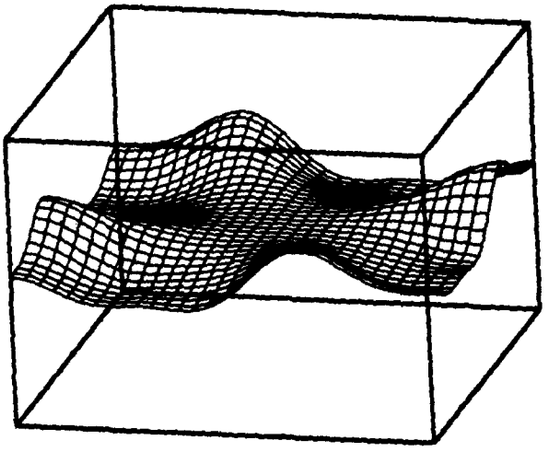

Figure 10. Spatial variation of the other solution along the m branch in Figure 7 at $t/2\pi = 3/4 \pm k$, $k = 0, 1, 2, \ldots$. The parameters are $\xi = 1$, $m = 1$, $n = 3$, $\varepsilon = 0.1$, $A_{11} = 1/\sqrt{2}$, and $A_{12} = -1/\sqrt{2}$.

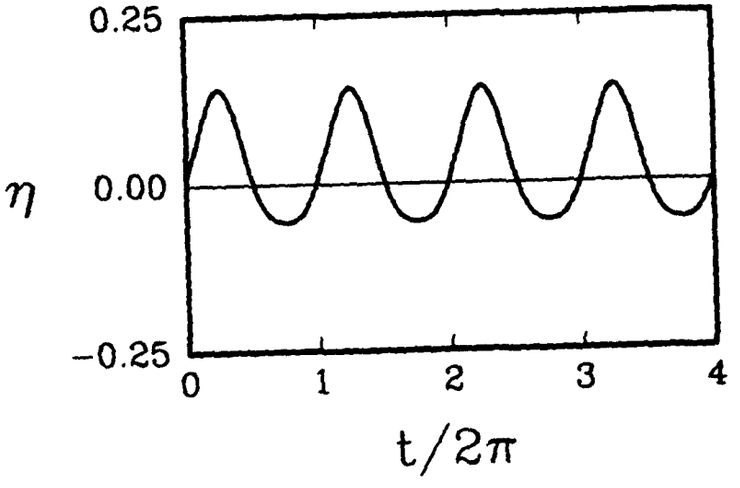

Figure 11a. Time series of the wave height in the left front corner ($\bar{x} = \bar{z} = 0$) of the vessel in Figure 8. The parameters are $\xi = 1.$, $m = 1$, $n = 3$, $\varepsilon = 0.1$, $A_{11} = 1.$, and $A_{12} = 0$.

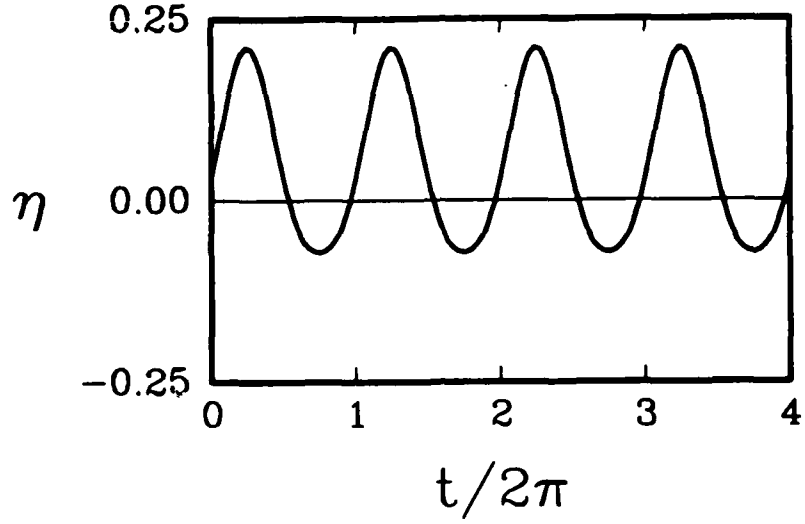

Figure 11b. Time series of the wave height in the left front corner ($\bar{x} = \bar{z} = 0$) of the vessel in Figure 9. The parameters are $\xi = 1.$, $m = 1$, $n = 3$, $\epsilon = 0.1$, $A_{11} = 1/\sqrt{2}$, and $A_{12} = 1/\sqrt{2}$.

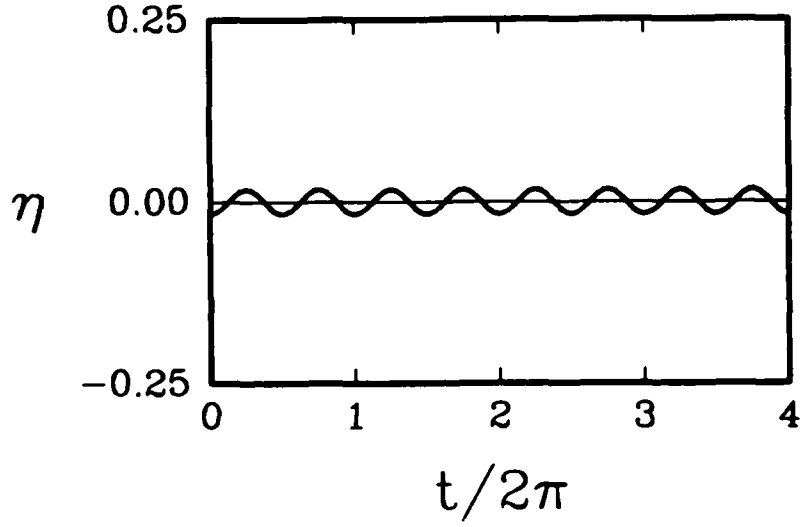

Figure 11c. Time series of the wave height in the left front corner ($\bar{x} = \bar{z} = 0$) of the vessel in Figure 10. The parameters are $\xi = 1.$, $m = 1$, $n = 3$, $\epsilon = 0.1$, $A_{11} = 1/\sqrt{2}$, and $A_{12} = -1/\sqrt{2}$.

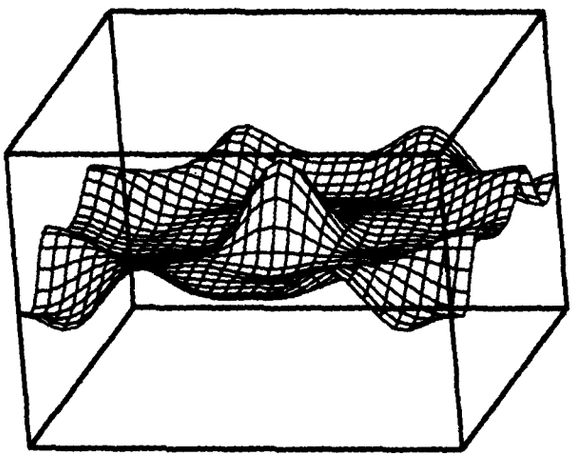

Figure 12. An example of the wave form on a mixed branch emitted by a double eigenvalue for $m = 2$, $n = 4$, $\xi = 1$, $\varepsilon = 0.1$, and $A_{11} = A_{12} = 1/\sqrt{2}$. The fact that m is even and n is a multiple of m produces a greater degree of symmetry in the mixed mode.

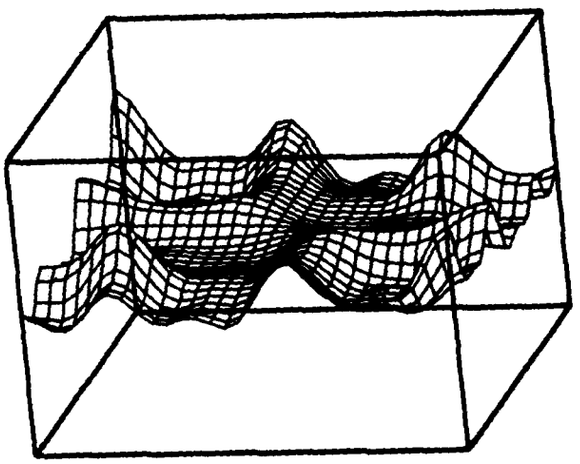

Figure 13. An example wave field illustrating the spatial complexity which can occur. The solution is on a mixed branch emitted by a double eigenvalue for $m = 1$, $n = 5$, $\xi = 1.$, $\varepsilon = 0.1$, and $A_{11} = A_{12} = 1/\sqrt{2}$.

4. The Secondary Bifurcation Points

In this section, solutions which bifurcate from the primary branches found in Section 2 are sought. Therefore a perturbation is added to the known primary branch solution,

$$\phi^* = \varepsilon^* \Phi + \phi \tag{4.1a}$$

$$\eta^* = \varepsilon^* h + \eta \tag{4.1b}$$

The expressions (4.1) are substituted into the governing set of equations and boundary conditions (2.1) - (2.4) and linearized. The equations independent of ϕ and η were analyzed in Section 2. The linear problem for ϕ and η is

$$\frac{\partial^2 \phi}{\partial x^2} + \frac{\partial^2 \phi}{\partial y^2} + \xi^2 \frac{\partial^2 \phi}{\partial z^2} = 0 \tag{4.2}$$

$$\frac{\partial \phi}{\partial x} \to 0 \quad \text{at} \quad x = \pm 1/2 \tag{4.3a}$$

$$\frac{\partial \phi}{\partial y} \to 0 \quad \text{as} \quad y \to -\infty \tag{4.3b}$$

$$\frac{\partial \phi}{\partial z} \to 0 \quad \text{at} \quad z = \pm 1/2 \tag{4.3c}$$

and on $y = \varepsilon^* h(x,z,t)$,

$$\omega^* \frac{\partial \eta}{\partial t} + \varepsilon^* \frac{\partial \Phi}{\partial x} \frac{\partial \eta}{\partial x} + \varepsilon^* \frac{\partial h}{\partial x} \frac{\partial \phi}{\partial x} + \varepsilon^* \xi^2 \left[\frac{\partial \Phi}{\partial z} \frac{\partial \eta}{\partial z} + \frac{\partial h}{\partial z} \frac{\partial \phi}{\partial z} \right] - \frac{\partial \phi}{\partial y} = 0 \tag{4.4}$$

and

$$\omega^* \frac{\partial \phi}{\partial t} + \varepsilon^* \left[\frac{\partial \Phi}{\partial x} \frac{\partial \phi}{\partial x} + \frac{\partial \Phi}{\partial y} \frac{\partial \phi}{\partial y} + \xi^2 \frac{\partial \Phi}{\partial z} \frac{\partial \phi}{\partial z} \right] + \eta = 0 \tag{4.5}$$

This is a linear differential eigenvlue problem with known nonconstant coefficients. However, the specific value of ε^* where the secondary bifurcation takes place is sought. Therefore ε^* is the eigenvalue. Since ε^* appears non-linearly, it is a non-linear, in the parameter, eigenvalue problem. This does not pose serious complications as methods for the solution of this type of problem are known [9]. However, there is the

further complication that ε^* is responsible for the size of the domain. The qualitative shape of the domain is known since $h(x,z,t)$ is a known function, but the precise amount of $h(x,z,t)$ is the unknown eigenvalue. This is to be contrasted with the original eigenvalue problem in Section 2 where ω^* was the eigenvalue, ε^* was a variable parameter, and the shape of the free surface, and hence the domain, was an unknown function.

To solve this eigenvalue problem, the conjecture of Bauer, Keller, and Reiss, that the secondary bifurcation occurs in the neighborhood of multiple eigenvalues, is used.

For brevity, the analysis is undertaken in the neighborhood of $\xi = 1$ (a square cross-section). It is expected that a similar analysis will hold in the neighborhood of other values of ξ at which double eigenvalues occur.

It was shown in Section 3 that for $\xi = 1$ there is a double eigenvalue for every pair (m,n) such that $m \neq n$. At the double eigenvalue the bifurcation point corresponds to

$$\lambda_0 = \pi(m^2 + n^2)^{1/2} \tag{4.6}$$

for any (m,n) such that $m \neq n$, and in the neighborhood of $\xi = 1$ this double eigenvalue splits into two primary branches

$$\lambda_{m,n} = \pi(m^2 + \xi^2 n^2)^{1/2} \tag{4.7}$$

and

$$\lambda_{n,m} = \pi(n^2 + \xi^2 m^2)^{1/2} \tag{4.8}$$

The neighborhood of $\xi = 1$ is measured by the small parameter μ, defined by

$$\xi = 1 + \frac{\tau\mu^2}{2} \quad \text{where} \quad \tau = \text{sign}\,(\xi-1) = \pm 1 \tag{4.9}$$

Following the conjecture of Bauer, Keller, and Reiss that the secondary bifurcation disappears at the double eignvalue, the point ε^* on the primary brnches where secondary bifurcation takes place is expressed as

$$\varepsilon^*(\mu) = b_0\mu + b_1\mu + \ldots \tag{4.10}$$

with (4.9) and (4.10) the solutions on the primary branch, derived in Section 2, can be re-expressed in terms of μ,

$$\Phi = \psi_0 + \mu\psi_1 + \ldots \tag{4.11a}$$

$$h = h_0 + \mu h_1 + \ldots \tag{4.11b}$$

$$\omega^* = \omega_0 + \mu^2\omega_2 + \ldots \tag{4.12}$$

The analysis is undertaken separately on the two branches, $\lambda_{m,n}$ and $\lambda_{n,m}$ after splitting. The necessary details for the analysis along the branch $\lambda_{m,n}$ is given, and the result only will be stated for the $\lambda_{n,m}$ branch. Along the primary branch corresponding to $\lambda_{m,n}$,

$$\lambda_{m,n} = \lambda_0 \left[1 + \frac{\tau\beta_n^2}{2\lambda_0^2}\mu^2 + \ldots\right] \tag{4.13}$$

where λ_0 is given in equation (4.6). The terms in the expansion (4.12) are given by

$$\omega_0 = \lambda_0^{1/2} \tag{4.14a}$$

and

$$\omega_2 = \frac{\tau\beta_n^2}{4\omega_0^3} + b_0^2\omega_0\left[\frac{-\omega_0^4}{8} - \frac{3(\alpha_m^4 + \beta_n^4)}{32\omega_0^4}\right]$$

$$+ b_0^2\left[\frac{\alpha_m^4}{4\omega_0(2\omega_0^2 - \beta_n)} + \frac{\beta_n^4}{4\omega_0(2\omega_0^2 - \alpha_m)}\right] \tag{4.14b}$$

and the terms in the wave height expansion (4.11b) are given by

$$h_0 = \cos \alpha_m\bar{x} \cos \beta_n\bar{z} \sin t \tag{4.15a}$$

$$h_1 = (D_{11} + D_{12} \cos 2t) \cos 2\alpha_m\bar{x} + (D_{13} + D_{14} \cos 2t) \cos 2\beta_n\bar{z}$$

$$+ (D_{15} + D_{16} \cos 2t) \cos 2\alpha_n\bar{x} \cos 2\beta_n\bar{z} \tag{4.15b}$$

where $\alpha_m = m\pi$, $\beta_n = n\pi$, $\bar{x} = x + 1/2$, $\bar{z} = z + 1/2$, and

$$D_{11} = \frac{b_0 \alpha_m^2}{8\omega_o^2}, \tag{4.16a}$$

$$D_{12} = \frac{-b_0(\omega_0^4 + \beta_n^2)}{8\omega_0^2} - \frac{b_0\beta_n^2}{2(\alpha_m - 2\omega_0^2)} \tag{4.16b}$$

$$D_{13} = \frac{b_0\beta_n^2}{8\omega_0^2} \tag{4.16c}$$

$$D_{14} = \frac{-b_0(\omega_0^4 + \alpha_m^2)}{8\omega_0^2} - \frac{b_0\alpha_m^2}{2(\beta_n - 2\omega_0^2)} \tag{4.16d}$$

$$D_{15} = b_0\omega_0^2/8 \tag{4.16e}$$

$$D_{16} = - b_0\omega_0^2/8 \tag{4.16f}$$

and a similar expression is found for Φ in (4.11a). Substituting the expressions (4.9), (4.10), (4.11) into the eigenvalue problem (4.2) - (4.5) and postulating that

$$\phi = \mu\phi_1 + \mu^2\phi_2 + \ldots \tag{4.17a}$$

$$\eta = \mu\eta_1 + \mu^2\eta_2 + \ldots \tag{4.17b}$$

expanding the free surface boundary conditions in a Taylor series, and equating terms proportional to like powers of μ to zero, results in the sequence of problems,

$$\frac{\partial^2\phi_j}{\partial x^2} + \frac{\partial^2\phi_j}{\partial y^2} + \frac{\partial^2\phi_j}{\partial z^2} = T_j \tag{4.18}$$

$$\frac{\partial\phi_j}{\partial x} = 0 \quad \text{at} \quad x = \pm 1/2 \tag{4.19a}$$

$$\frac{\partial\phi_j}{\partial y} \to 0 \quad \text{as} \quad y \to -\infty \tag{4.19b}$$

$$\frac{\partial\phi_j}{\partial z} = 0 \quad \text{at} \quad z = \pm 1/2 \tag{4.19c}$$

$$\omega_0 \frac{\partial \phi_j}{\partial t} + \eta_j = R_j \tag{4.20}$$

$$\omega_0 \frac{\partial \eta_j}{\partial t} - \frac{\partial \phi_j}{\partial y} = S_j \tag{4.21}$$

for $j = 1, 2, \ldots$.

In addition to the obvious differences between the R_j and S_j appearing here and those in the previous sets, there is also the addition of the inhomogeneous term in the governing equation (4.18). However $T_1 = 0$, $T_2 = 0$, and $T_3 = -\tau \frac{\partial^2 \phi_1}{\partial z^2}$.

Noting that $R_1 = S_1 = T_1 = 0$, and the fact that ω_0 corresponds to a double eigenvalue, the first order solution is

$$\eta_1(x,z,t) = [A_{11}\cos \alpha_m \bar{x} \cos \beta_n \bar{z} + A_{12}\cos \beta_n \bar{x} \cos \alpha_m \bar{z}] \tag{4.22}$$

and

$$\phi_1(x,y,z,t) = \omega_0^{-1}[A_{11}\cos \alpha_m \bar{x} \cos \beta_n \bar{z} + A_{12}\cos \beta_n \bar{x} \cos \alpha_m \bar{z}]e^{\omega_0^2 y} \cos t \tag{4.23}$$

For definitness in the normalization, the following relation is taken between A_{11} and A_{12},

$$A_{11}^2 + A_{12}^2 = 1 \tag{4.24}$$

with the relative values of A_{11} and A_{12} to be determined at higher order.

Before proceeding to higher order, it is noted that the homogeneous problem has a double eigenvalue. Therefore two solvability conditions are needed at each order. The general form of the solvability condition, given in Appendix II, is used. Substitution of the known solutions into R_2 and S_2 the second order solution is found to be,

$$\begin{aligned}\eta_2(x,z,t) = {} & C_{20} b_0 A_{11} \cos 2t \\ & + [B_{21} + C_{21}\cos 2t]\, b_0 A_{11} \cos 2\alpha_m \bar{x} \\ & + [B_{22} + C_{22}\cos 2t]\, b_0 A_{11} \cos 2\beta_n \bar{z} \\ & + [B_{23} + C_{23}\cos 2t]\, b_0 A_{11} \cos 2\alpha_m \bar{x} \cos 2\beta_n \bar{z}\end{aligned}$$

$$+ [B_{24} + C_{24}\cos 2t]\, b_0 A_{12} \cos(\alpha_m - \beta_n)\bar{x} \cos(\alpha_m - \beta_n)\bar{z}$$

$$+ [B_{25} + C_{25}\cos 2t]\, b_0 A_{12} \cos(\alpha_m + \beta_n)\bar{x} \cos(\alpha_m + \beta_n)\bar{z}$$

$$+ C_{26} b_0 A_{12} \cos 2t\, [\cos(\alpha_m - \beta_n)\bar{x} \cos(\alpha_m + \beta_n)\bar{z}$$

$$+ \cos(\alpha_m + \beta_n)\bar{x} \cos(\alpha_m - \beta_n)\bar{z}] \qquad (4.25)$$

and

$$\phi_2(x,y,z,t) = A_{00} b_0 A_{11} t + A_{20} b_0 A_{11} \sin 2t$$

$$+ b_0 A_{11} \sin 2t\, [A_{21} e^{2\alpha_m y} \cos 2\alpha_m \bar{x} + A_{22} e^{2\beta_n y} \cos 2\beta_n \bar{z}$$

$$+ A_{23} e^{\omega_0^2 y} \cos 2\alpha_m \bar{x} \cos 2\beta_n \bar{z}]$$

$$+ b_0 A_{12} \sin 2t [A_{24} \cos(\alpha_m - \beta_n)\bar{x} \cos(\alpha_m - \beta_n)\bar{z} \exp[\sqrt{2}|\alpha_m - \beta_n|y]$$

$$+ A_{25} \cos(\alpha_m + \beta_n)\bar{x} \cos(\alpha_m + \beta_n)\bar{z} \exp[\sqrt{2}(\alpha_m + \beta_n)y]$$

$$+ A_{26} \cos(\alpha_m - \beta_n)\bar{x} \cos(\alpha_m + \beta_n)\bar{z} \exp[\sqrt{2}\,\omega_0^2 y]$$

$$+ A_{26} \cos(\alpha_m + \beta_n)\bar{x} \cos(\alpha_m - \beta_n)\bar{z} \exp[\sqrt{2}\,\omega_0^2 y]] \qquad (4.26)$$

The coefficients A_{2j}, B_{2j}, and C_{2j} are given in Appendix IV. The term $C_{20} b_0 A_{11} \cos 2t$ in the expression for η_2 in (4.25) is indicative of non-conservation of mass. Conservation of mass requires that

$$\int_{-1/2}^{1/2} \int_{-1/2}^{1/2} \eta_j(x,z,t)\,dx\,dz = 0 \qquad (4.27)$$

which is not satisfied by the term mentioned. However, the solvability condition, at the next order requires that the product $b_0 A_{11}$ is always zero, which alleviates this problem.

Substitution of the known solutions and application of the general solvability condition at third order results in the bifurcation equations,

$$b_0^2 A_{11} = 0 \tag{4.28}$$

$$\left[-\frac{(\alpha_m^2 - \beta_n^2)\tau}{2\omega_0^4} - a_3 b_0^2 \right] A_{12} = 0 \tag{4.29}$$

which along with the normalizaiton condition

$$A_{11}^2 + A_{12}^2 = 1 \tag{4.30}$$

form a set of three equations for the three unknowns A_{11}, A_{12}, and b_0. The term a_3 is given by

$$\begin{aligned} a_3 = {} & \frac{5\omega_0^4}{32} + \frac{3(\alpha_m^4 + \beta_n^4)}{8\omega_0^4} + \frac{3\omega_0^2}{16\sqrt{2}} \left[|\alpha_m - \beta_n| + (\alpha_m + \beta_n) \right] \\ & + \frac{\alpha_m \beta_n}{2\sqrt{2}\,\omega_0^2} \left[|\alpha_m - \beta_n| - (\alpha_m + \beta_m) \right] \\ & - \frac{\alpha_m^4}{2\omega_0^2(2\omega_0^2 - \beta_n)} - \frac{\beta_n^4}{2\omega_0^2(2\omega_0^2 - \alpha_m)} \\ & - \frac{7}{32\sqrt{2}} \left[\frac{|\alpha_m - \beta_n|(3\omega_0^4 + 8\alpha_m\beta_n)}{[4\omega_0^2 - \sqrt{2}|\alpha_m - \beta_n|]} + \frac{(\alpha_m + \beta_n)(3\omega_0^4 - 8\alpha_m\beta_n)}{[4\omega_0^2 - \sqrt{2}(\alpha_m + \beta_n)]} \right] \end{aligned} \tag{4.31}$$

It has not been proved that this expression, a_3, is positive definite but numerical evaluation, with m,n ranging from 1 to 10, showed this to be the case. The solutions to (4.28) - (4.30) are

$$\text{Case I:} \quad b_0 = 0, \quad A_{11} = 1, \quad A_{12} = 0 \tag{4.32}$$

$$\text{Case II:} \quad b_0 = \pm \sqrt{\frac{-(\alpha_m^2 - \beta_n^2)\tau}{2a_3\omega_0^4}}, \quad A_{11} = 0, \quad A_{12} = 1 \tag{4.33}$$

The solution is (4.32) is of little interest. It merely points out that the basic solution bifurcates from the primary branch. In (4.33) the solution for the secondary bifurcation on branch $\lambda_{m,n}$ is given. The $\pm$ sign in (4.33) shows that the bifurcation takes place in both the upper and lower half planes $(\pm \varepsilon)$. The jump to the $A_{12} \neq 0$ solution is often referred to as mode jumping because the solution acquired on the secondary branch is qualitatively different from that on the primary branch. The radical in (4.33), with the conjecture that $a_3 > 0$, requires that $(\alpha_m - \beta_m)\tau < 0$ for secondary bifurcation to occur on branch $\lambda_{m,n}$.

A similar analysis, to that given for the $\lambda_{m,n}$ branch, results in the following bifurcation equations for the $\lambda_{n,m}$ branch,

$$\left[\frac{(\alpha_m^2 - \beta_n^2)\tau}{2\omega_0^4} - a_3 b_0^2\right] A_{11} = 0 \tag{4.34}$$

$$b_0^2 A_{12} = 0 \tag{4.35}$$

which along with (4.30) provides three equations for the three unknowns. For convenience, define $\varepsilon_{m,n}$ to be the point of secondary bifurcation on the $\lambda_{m,n}$ branch and $\varepsilon_{n,m}$ to be the point of secondary bifurcation on the $\lambda_{n,m}$ branch, where

$$\varepsilon_{m,n}(\mu) = b_{m,n}\mu + O(\mu^2) \tag{4.36}$$

$$\varepsilon_{n,m}(\mu) = b_{n,m}\mu + O(\mu^2) \tag{4.37}$$

Equation (4.33) and (4.34) show that (retaining only the positive branch for brevity),

$$b_{m,n} = \sqrt{\frac{-(\alpha_m^2 - \beta_n^2)\tau}{2a_3\omega_0^4}} \tag{4.38}$$

$$b_{n,m} = \sqrt{\frac{(\alpha_m^2 - \beta_n^2)\tau}{2a_3\omega_0^4}} \tag{4.39}$$

The secondary bifurcation phenomena may be summarized as follows.

When $\mu = 0$ and $\xi = 1$ there is a double eigenvalue $\lambda_0 = (\alpha_m^2 + \beta_n^2)^{1/2}$ for every pair (m,n) such that $m \neq n$. As ξ is varied from $\xi = 1$ by an amount $\xi = 1 + \frac{1}{2}\tau\mu^2$, the double bifurcation point splits into two primary bifurcation points,

$$\lambda_{m,n} = (\alpha_m^2 + \xi^2\beta_n^2)^{1/2} \tag{4.40a}$$

$$\lambda_{n,m} = (\beta_n^2 + \xi^2\alpha_m^2)^{1/2} \tag{4.40b}$$

According to (4.36) - (4.39) a secondary bifurcation tkes place on one - and only one at a time - branch. Noting that $\tau = \text{sign}\,(\xi - 1)$ and that the radical in (4.38) and (4.39) must be positive for secondary bifurcation, the branch on which the secondary bifurcation takes place is

$$\text{If } \xi > 1 \text{ and } \alpha_m > \beta_n \text{ then on } \lambda_{n,m} \tag{4.41a}$$

$$\text{If } \xi > 1 \text{ and } \alpha_m < \beta_n \text{ then on } \lambda_{m,n} \tag{4.41b}$$

$$\text{If } \xi < 1 \text{ and } \alpha_m > \beta_n \text{ then on } \lambda_{m,n} \tag{4.41c}$$

$$\text{If } \xi < 1 \text{ and } \alpha_m < \beta_n \text{ then on } \lambda_{n,m} \tag{4.41d}$$

These results suggest the following. As ξ departs from $\xi = 1$, the split primary bifurcation points move away from the double point. When $\xi > 1$ they both move to the right, and when $\xi < 1$ they both move to the left. However, in all four cases (4.41), the secondary bifurcation takes place on the branch which is emitted, after splitting, by the largest, in magnitude, of the two bifurcation points, regardless of the sign of τ.

Based on physical and numerical grounds the size of the ξ neighborhood, in which secondary bifurcation may take place, can be estimated. Schwartz and Whitney [10], in their analysis of two-dimensional standing waves, in a fluid of infinite depth, estimated the highest wave to occur at $\varepsilon \sim 0.2$ (the scaling here is different, dividing their result by π provides congruence with this work). This two-dimensional result may be used as an estimate of the relevant three-dimensional parameter. Numerical evaluation of the expression for b_0 gives a value of $b_0 \sim 0.18$ for $m = 1$, $n = 2$, and for all

combinations of m,n with m,n ranging over 1 to 10, the value of b_0 is of smaller magnitude. This suggests an upper bound for μ of $\mu \sim 1$. Obviously the perturbation scheme is valid only as $\mu \to 0$. But the implication is that the neighborhood around $\xi = 1$ in which secondary bifurcation takes place may be substantial. Therefore the range of aspect ratios at which secondary bifurcation may take place, at some value of the wave amplitude, is large enough that the irregular waves produced on these branches should occur quite often in vessels of rectangular cross-section. In the next section the solutions along the secondary branches will be found.

5. The Solution Along the Secondary Branch

After the splitting process, a secondary bifurcation point occurs on one of the two resulting primary branches. By expanding in the neighborhood of this point, an asymptotic representation of the solution along the secondary branch may be found. Assume the parameters are such that the secondary bifurcation point occurs on the $\lambda_{m,n}$ branch. A similar expansion can be performed if the secondary bifurcation point occurs on the $\lambda_{n,m}$ branch. The governing equations and boundary conditions are given in expressions (2.1) - (2.4). The variables have the following form,

$$\phi^* = \varepsilon\Phi + \phi \tag{5.1a}$$

$$\eta^* = \varepsilon h + \eta \tag{5.1b}$$

$$\omega^* = \omega + \Omega \tag{5.1c}$$

where Φ, h, and ω correspond to solutions on the primary branch and ϕ, η, and Ω correspond to solutions on the secondary branch. The primary branch solutions were found in section 2. The problem for ϕ, η, and Ω is given by

$$\frac{\partial^2\phi}{\partial x^2} + \frac{\partial^2\phi}{\partial y^2} + \xi^2\frac{\partial^2\phi}{\partial z^2} = 0 \tag{5.2a}$$

$$\frac{\partial\phi}{\partial x} = 0 \quad \text{at} \quad x = \pm\,{}^1\!/_2 \tag{5.2b}$$

$$\frac{\partial\phi}{\partial y} \to 0 \quad \text{as} \quad y \to -\infty \tag{5.2c}$$

$$\frac{\partial\phi}{\partial z} = 0 \quad \text{at} \quad z = \pm\,{}^1\!/_2 \tag{5.2d}$$

and on $y = \varepsilon h + \eta$

$$(\omega + \Omega)\frac{\partial\eta}{\partial t} - \frac{\partial\phi}{\partial y} + \varepsilon\left\{\frac{\partial\Phi}{\partial x}\frac{\partial\eta}{\partial x} + \xi^2\frac{\partial\Phi}{\partial z}\frac{\partial\eta}{\partial z} + \frac{\partial h}{\partial x}\frac{\partial\phi}{\partial x} + \xi^2\frac{\partial h}{\partial z}\frac{\partial\phi}{\partial\zeta}\right\}$$

$$+ \frac{\partial\phi}{\partial x}\frac{\partial\eta}{\partial x} + \xi^2\frac{\partial\phi}{\partial z}\frac{\partial\eta}{\partial z} = -\varepsilon(\omega + \Omega)\frac{\partial h}{\partial t} - \varepsilon^2\left\{\frac{\partial\Phi}{\partial x}\frac{\partial h}{\partial x} + \xi^2\frac{\partial\Phi}{\partial z}\frac{\partial h}{\partial z}\right\} - \varepsilon\frac{\partial\Phi}{\partial y} \tag{5.3a}$$

and

$$(\omega + \Omega)\frac{\partial\phi}{\partial t} + \eta + \varepsilon\left\{\frac{\partial\Phi}{\partial x}\frac{\partial\phi}{\partial x} + \frac{\partial\Phi}{\partial y}\frac{\partial\phi}{\partial y} + \xi^2\frac{\partial\Phi}{\partial z}\frac{\partial\phi}{\partial z}\right\} + \frac{1}{2}\nabla\phi\cdot\nabla\phi =$$

$$-\varepsilon(\omega + \Omega)\frac{\partial\Phi}{\partial t} - \varepsilon h - \frac{\varepsilon^2}{2}\nabla\Phi\cdot\nabla\Phi \qquad (5.3b)$$

The free surface boundary conditions satisfied by Φ and h are subtracted from (5.3a) and (5.3b) after expansion of these conditions in Taylor series about $y = 0$. A small parameter, ν, is defined as a measure of the distance from the secondary bifurcation point. The known primary branch solutions are

$$\varepsilon = b_{m,n}\mu + 0(\mu^2) \qquad (5.4a)$$

$$\Phi = \psi_0 + \mu\psi_1 + 0(\mu^2) \qquad (5.4b)$$

$$h = h_0 + \mu h_1 + 0(\mu^2) \qquad (5.4c)$$

$$\omega = \omega_0 + \mu^2\omega_2 + 0(\mu^3) \qquad (5.4d)$$

with $b_{m,n}$ given in (4.38), and the terms in (5.4c) and (5.4d) are given in (4.14a) through (4.15b). The unknown solutions along the secondary branch are postulated to have the following form

$$\phi = \nu\phi_1 + \nu^2\phi_2 + \ldots \qquad (5.5a)$$

$$\eta = \nu\eta_1 + \nu^2\eta_2 + \ldots \qquad (5.5b)$$

$$\Omega = \nu\Omega_1 + \nu^2\Omega_2 + \ldots \qquad (5.5c)$$

Substituting (5.4) - (5.5) into the governing equations and boundary conditions, (5.2) and (5.3), expanding the free surface boundary conditions in a Taylor series about the equilibrium solution, and equating terms proportional to like powers of ν to zero, results in a sequence of boundary value problems for the ϕ_i, η_i, and Ω_i. However, each

of these boundary value problems is also a function of μ. Therefore the functions ϕ_i, η_i, and Ω_i are expanded in terms proportional to powers of μ,

$$\phi_i = \mu\phi_{i1} + \mu^2\phi_{i2} + \ldots \tag{5.6}$$

$$\eta_i = \mu\eta_{i1} + \mu^2\eta_{i2} + \ldots \tag{5.7}$$

$$\Omega_i = \Omega_{i0} + \mu\Omega_{i1} + \mu^2\Omega_{i2} + \ldots \tag{5.8}$$

The substitution of these expressions results in an additional subdivision of boundary value problems. The analysis, although straightforward, is lengthy and the details will not be presented.

The first order (in ν) problem results in $\Omega_1 = 0$, and

$$\phi_1 = \mu\phi_{11} + \mu^2\phi_{12} + 0(\mu^3) \tag{5.9}$$

$$\eta_1 = \mu\eta_{11} + \mu^2\eta_{12} + 0(\mu^3) \tag{5.10}$$

where

$$\phi_{11} = \omega_0^{-1}\cos\beta_n\bar{x}\cos\alpha_m\bar{z}\, e^{\omega_0^2 y}\cos t \tag{5.11}$$

$$\eta_{11} = \cos\beta_n\bar{x}\cos\alpha_m\bar{z}\sin t \tag{5.12}$$

where the parameters are as previously defined, and

$$\begin{aligned}\phi_{12} = {} & A_{121}\cos(\alpha_m - \beta_n)\bar{x}\cos(\alpha_m - \beta_n)\bar{z}\exp[\sqrt{2}|\alpha_m - \beta_n|y]\sin 2t \\ & + A_{122}\cos(\alpha_m + \beta_n)\bar{x}\cos(\alpha_m + \beta_n)\bar{z}\exp[\sqrt{2}(\alpha_m + \beta_n)y]\sin 2t \\ & + A_{123}\cos(\alpha_m - \beta_n)\bar{x}\cos(\alpha_m + \beta_n)\bar{z}\exp[\sqrt{2}\,\omega_0^2 y]\sin 2t \\ & + A_{123}\cos(\alpha_m + \beta_n)\bar{x}\cos(\alpha_m - \beta_n)\bar{z}\exp[\sqrt{2}\,\omega_0^2 y]\sin 2t\end{aligned} \tag{5.13}$$

and

$$\begin{aligned}\eta_{12} = {} & [B_{121} + C_{121}\cos 2t]\cos(\alpha_m - \beta_n)\bar{x}\cos(\alpha_m - \beta_n)\bar{z} \\ & + [B_{122} + C_{122}\cos 2t]\cos(\alpha_m + \beta_n)\bar{x}\cos(\alpha_m + \beta_n)\bar{z} \\ & + [B_{123} + C_{123}\cos 2t]\cos(\alpha_m - \beta_n)\bar{x}\cos(\alpha_m + \beta_n)\bar{z} \\ & + [B_{123} + C_{123}\cos 2t)\cos(\alpha_m + \beta_n)\bar{x}\cos(\alpha_m - \beta_m)\bar{z}\end{aligned} \tag{5.14}$$

and the coefficients in ϕ_{12} and η_{12} are given in Appendix V.

The problem of $O(\nu^2)$ yields the following results,

$$\Omega_2 = \Omega_{20} + \mu\Omega_{21} + \mu^2\Omega_{22} + O(\mu^3) \tag{5.15}$$

$$\phi_2 = \mu\phi_{21} + \mu^2\phi_{22} + O(\mu^3) \tag{5.16}$$

$$\eta_2 = \mu\eta_{21} + \mu^2\eta_{22} + O(\mu^3) \tag{5.17}$$

where it has been found that $\Omega_{20} = \Omega_{21} = 0$,

$$\Omega_{22} = -\frac{(28 - 9\sqrt{2})}{(4 - \sqrt{2})}\frac{\omega_0^5}{32} - \frac{3\alpha_m^2\beta_n^2}{16\omega_0^3} + \frac{(\alpha_m + \beta_n)^4}{8\omega_0[4\omega_0^2 - \sqrt{2}|\alpha_m - \beta_n|]} + \frac{(\alpha_m - \beta_n)^4}{8\omega_0[4\omega_0^2 - \sqrt{2}(\alpha_m + \beta_n)]}, \tag{5.18}$$

$\phi_{21} = \eta_{21} = 0$, and

$$\phi_{22} = A_{221}\cos 2\beta_n\bar{x}\, e^{2\beta_n y}\sin 2t + A_{222}\cos 2\alpha_m\bar{z}\, e^{2\alpha_m y}\sin 2t + A_{223}\cos 2\beta_n\bar{x}\cos 2\alpha_m\bar{z}\, e^{2\omega_0^2 y}\sin 2t \tag{5.19}$$

and

$$\eta_{22} = (B_{221} + C_{221}\cos 2t)\cos 2\beta_n\bar{x} + (B_{222} + C_{222}\cos 2t)\cos 2\alpha_m\bar{z} + (B_{223} + C_{223}\cos 2t)\cos 2\beta_n\bar{x}\cos 2\alpha_m\bar{z} \tag{5.20}$$

The coefficients in (5.19) and (5.20) are also given Appendix V.

The result (5.18) provides the expression for the frequency along the secondary branch. In the limit as $\nu \to 0$ and $\mu \to 0$ the complete expression for the frequency is

$$\omega^* = \omega_0 + \mu^2\omega_2 + \mu^2\nu^2\Omega_{22} + O(\mu^3, \nu^3) \tag{5.21}$$

Since Ω_{22} is proportional to quadratic terms, the sign of Ω_{22} determines whether the bifurcation from the secondary bifurcation points is subcritical or supercritical. It has not been proved, but numerical evaluation of the expression for Ω_{22} suggests that it is negative for all values of m and n. Therefore, as the solution moves from the primary to the secondary branch the frequency of oscillation decreases.

An example of this secondary bifurcation phenomena is given in Figure 14. In this particular example $m = 2$ and $n = 1$. The double bifurcation point, $\lambda_0^{1/2} \sim 2.65$, is given by the dashed line in the figure. This point is split by choosing $\mu = \frac{2}{3}$. With $\tau < 0$ the aspect ratio after splitting is $\xi = \frac{7}{9}$. Therefore the two primary bifurcation points become $\lambda_{2,1} \sim 2.6$ and $\lambda_{1,2} \sim 2.4$. For these parameters $b_0 \sim 0.18$. Therefore the secondary bifurcation takes place at $\varepsilon^* \sim 0.12$, on the $\lambda_{2,1}$ branch, and from this point the subcritical secondary branches are emitted.

The nature of the solutions on the secondary branch can be illustrated by the time series, for the wave height in the left front corner of the tank ($\bar{x} = \bar{z} = 0$), given in Figures 15a and 15b. The result corresponds to that given in Figure 14. In Figure 15a the wave height on the primary branch at the secondary bifurcation point ($\varepsilon = .12$, $\nu = 0$, $m = 2$, $n = 1$) is shown. In Figure 15b the solution is advanced along the secondary branch to $\nu = 0.08$.

The spatial nature of the solution on the secondary branches will be similar to the result found for the mixed modes emitted by the double eigenvalues. However a greater degree of complexity may be expected here due to the varying amount (through ν) of the "other" mode which is acquired on the secondary branch.

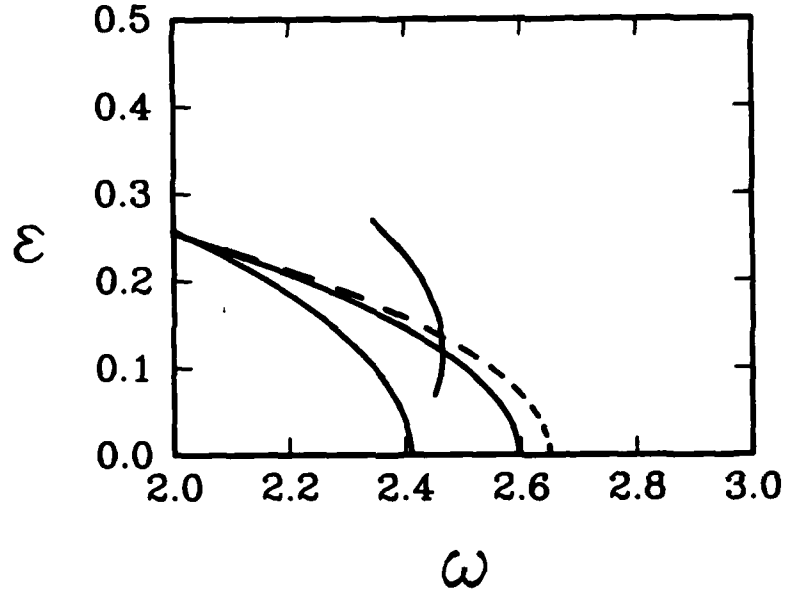

Figure 14. A bifurcation diagram with the occurrence of secondary bifurcation for $m = 2$ and $n = 1$. When $\xi = 1$ the pure branch emitted by the double eigenvalue is given by the dashed line. When ξ is perturbed to $\xi = 7/9$ the double eigenvalue splits and secondary bifurcation occurs on the $\lambda_{2,1}$ branch.

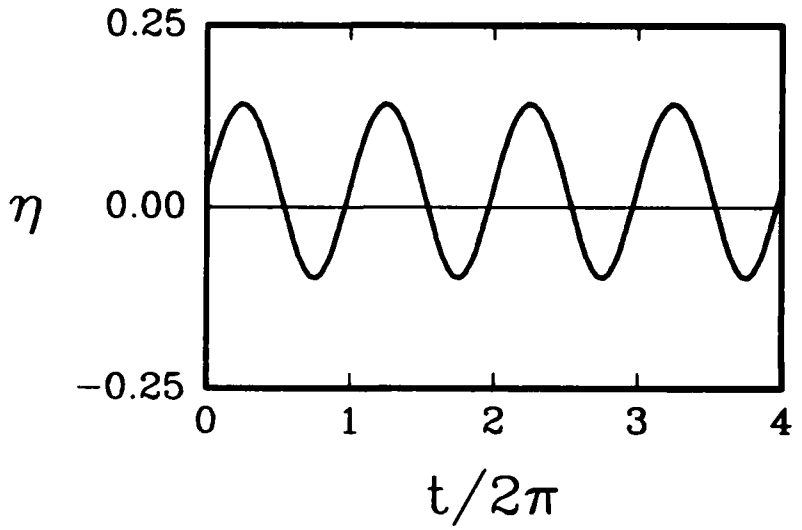

Figure 15a. Times series for the wave height corresponding to Figure 14. The parameters are $\xi = 7/9$, $m = 2$, $n = 1$, $\varepsilon = 0.12$, and $\nu = 0$. This is the solution on the primary branch near the secondary bifurcation point.

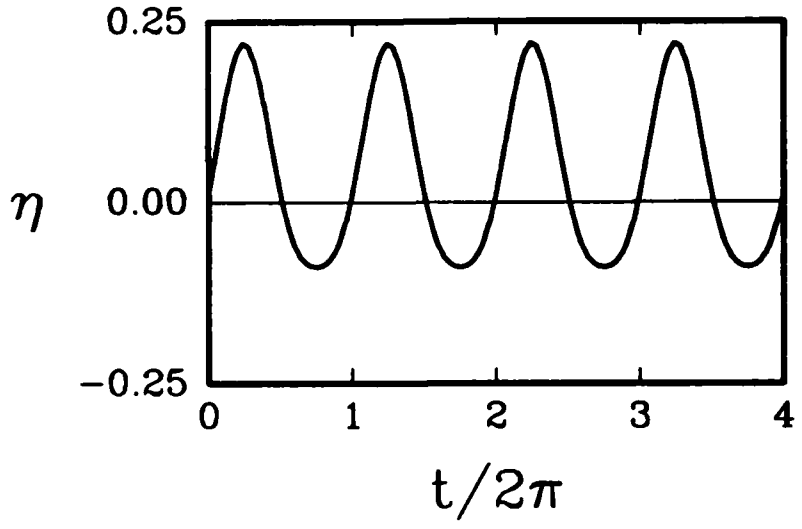

Figure 15b. Time series for the wave height corresponding to Figure 14. The parameters are $\xi = 7/9$, $m = 2$, $n = 1$, $\varepsilon = 0.12$, and $\nu = 0.08$. This is a solution on the secondary branch.

6. Remarks

It has been formally shown that multiple and secondary bifurcation of the wave fields occurs in partially filled vessels of rectangular cross section when the depth of the fluid is infinite. The many wave solutions depicted in this paper will likely occur often in nature. Unlike the buckling of plates and shells, for example, where the minimum eigenvalue is the most important, in the "sloshing" problem the band of frequencies, at which a vessel containing fluid might be excited, is relevant. Consider, for example, an ocean liner carrying liquid cargo steaming across the north Atlantic. The ship, and hence the cargo tanks, will be subjected to ocean waves containing a significant band of frequencies and amplitudes. It is likely, in fact, that even the most casual observer of waves in partially filled vessels of rectangular cross-section has witnessed wave fields of the type shown herein.

What about vessels with cross-sections other than rectangular? A basin with a triangular cross-section, for example, will have a multiple (triple?) eigenvalue when it is equilateral. Similarily, one can imagine that a star-shaped cross-section will also produce interesting possibilities.

A basin with a circular cross-section, such as a coffee cup, is however different. There is no relevant parameter such as an aspect ratio. An analogy can be found in the work of Cheo and Reiss [11] on the secondary buckling of circular plates. Their analysis showed that a different type of secondary bifurcation occurs in the buckling of plates with circular cross-section. In their case, the primary bifurcation was to an axisymmetric state, from which a secondary bifurcation to an asymmetric state was found. In the standing wave problem Mack [12] has found the primary bifurcation points to axisymmetric states for standing waves in a circular basin. It is possible that a secondary bifurcation from these primary states to asymmetric states may take place.

Appendix I

The nonlinear boundary conditions at the free surface, $y = \eta^*(x,z,t)$, are

$$\omega^* \frac{\partial \eta}{\partial t} + \frac{\partial \phi^*}{\partial x}\frac{\partial \eta^*}{\partial x} + \xi^2 \frac{\partial \phi^*}{\partial z}\frac{\partial \eta}{\partial z} - \frac{\partial \phi^*}{\partial y} = 0 \tag{I.1}$$

$$\omega^* \frac{\partial \phi^*}{\partial t} + \frac{1}{2}\left[\left(\frac{\partial \phi^*}{\partial x}\right)^2 + \left(\frac{\partial \phi^*}{\partial y}\right)^2 + \xi^2\left(\frac{\partial \phi^*}{\partial z}\right)^2\right] + \eta^* = 0 \tag{I.2}$$

If each of the unknown variables has a power series expansion in the amplitude

$$\phi^* = \varepsilon\phi_1 + \varepsilon^2\phi_2 + \ldots \tag{I.3a}$$

$$\eta^* = \varepsilon\eta_1 + \varepsilon^2\eta_2 + \ldots \tag{I.3b}$$

$$\omega^* = \sigma_0 + \varepsilon\sigma_1 + \varepsilon^2\sigma_2 + \ldots \tag{I.3c}$$

After expansion of (I.1) and (I.2) about $y = 0$, and substitution of (I.3), the following sequence of boundary conditions results

$$\sigma_0 \frac{\partial \eta_j}{\partial t} - \frac{\partial \phi_j}{\partial y} = R_j \tag{I.4}$$

$$\sigma_0 \frac{\partial \phi_j}{\partial t} + \eta_j = S_j \tag{I.5}$$

where

$$R_1 = 0 \tag{I.6}$$

$$R_2 = -\sigma_1 \frac{\partial \eta_1}{\partial t} - \frac{\partial \eta_1}{\partial x}\frac{\partial \phi_1}{\partial x} - \xi^2 \frac{\partial \eta_1}{\partial z}\frac{\partial \phi_1}{\partial z} + \eta_1 \frac{\partial^2 \phi_1}{\partial y^2} \tag{I.7}$$

$$\begin{aligned} R_3 = {} & -\sigma_1 \frac{\partial \eta_2}{\partial t} - \sigma_2 \frac{\partial \eta_1}{\partial t} - \frac{\partial \eta_1}{\partial x}\frac{\partial \phi_2}{\partial x} - \xi^2 \frac{\partial \eta_1}{\partial z}\frac{\partial \phi_1}{\partial z} \\ & - \frac{\partial \eta_2}{\partial x}\frac{\partial \phi_1}{\partial x} - \xi^2 \frac{\partial \eta_2}{\partial z}\frac{\partial \phi_1}{\partial z} + \eta_1 \frac{\partial^2 \phi_2}{\partial y^2} + \eta_2 \frac{\partial^2 \phi_1}{\partial y^2} \\ & + \frac{1}{2}\eta_1^2 \frac{\partial^3 \phi_1}{\partial y^3} - \eta_1\left[\frac{\partial \eta_1}{\partial x}\frac{\partial^2 \phi_1}{\partial x \partial y} + \xi^2 \frac{\partial \eta_1}{\partial z}\frac{\partial^2 \phi_1}{\partial y \partial z}\right] \end{aligned} \tag{I.8}$$

$$S_1 = 0 \tag{I.9}$$

$$S_2 = -\sigma_1 \frac{\partial \phi_1}{\partial t} - \frac{1}{2} \nabla\phi_1 \cdot \nabla\phi_1 - \sigma_0 \eta_1 \frac{\partial^2 \phi_1}{\partial y \partial t} \tag{I.10}$$

$$\begin{aligned} S_3 = &-\sigma_1 \frac{\partial \phi_2}{\partial t} - \sigma_2 \frac{\partial \phi_1}{\partial t} - \frac{\partial \phi_1}{\partial x}\frac{\partial \phi_2}{\partial x} - \frac{\partial \phi_1}{\partial y}\frac{\partial \phi_2}{\partial y} - \xi^2 \frac{\partial \phi_1}{\partial z}\frac{\partial \phi_2}{\partial z} \\ &- \sigma_0 \eta_1 \frac{\partial^2 \phi_2}{\partial y \partial t} - \sigma_0 \eta_2 \frac{\partial^2 \phi_1}{\partial y \partial t} - \sigma_1 \eta_1 \frac{\partial^2 \phi_1}{\partial y \partial t} \\ &- \eta_1 \left\{ \frac{\partial \phi_1}{\partial x}\frac{\partial^2 \phi_1}{\partial y \partial x} + \frac{\partial \phi_1}{\partial y}\frac{\partial^2 \phi}{\partial y^2} + \xi^2 \frac{\partial \phi_1}{\partial z}\frac{\partial^2 \phi_1}{\partial y \partial z} \right\} - \frac{1}{2}\eta^2 \sigma_0 \frac{\partial^3 \phi_1}{\partial y^2 \partial t} \end{aligned} \tag{I.11}$$

Appendix II

Inhomogeneous eigenvalue problems of the following type arise in the analysis

$$\frac{\partial^2 \phi}{\partial x^2} + \frac{\partial^2 \phi}{\partial y^2} + \xi^2 \frac{\partial^2 \phi}{\partial z^2} = f_1(x,y,z)\cos t \tag{II.1}$$

$$\frac{\partial \phi}{\partial x} = 0 \quad \text{at} \quad x = \pm 1/2 \tag{II.2}$$

$$\frac{\partial \phi}{\partial y} \to 0 \quad \text{as} \quad y \to -\infty \tag{II.3}$$

$$\frac{\partial \phi}{\partial z} = 0 \quad \text{at} \quad z = \pm 1/2 \tag{II.4}$$

$$\frac{\partial \phi}{\partial y} + \sigma_0^2 \frac{\partial^2 \phi}{\partial t^2} = f_2(x,z)\cos t \tag{II.5}$$

Other inhomogeneous terms with higher multiples of t occur and for them a similar analysis holds. The term proportional to cost is the most important. Define $\Phi(x,y,z,t) = \phi(x,y,z)\cos t$, then ϕ satisfies

$$\frac{\partial^2 \phi}{\partial x^2} + \frac{\partial^2 \phi}{\partial y^2} + \xi^2 \frac{\partial^2 \phi}{\partial z^2} = f_1(x,y,z) \tag{II.6}$$

$$\frac{\partial \phi}{\partial x} = 0 \quad \text{at} \quad x = \pm 1/2 \tag{II.7}$$

$$\frac{\partial \phi}{\partial y} \to 0 \quad \text{as} \quad y \to -\infty \tag{II.8}$$

$$\frac{\partial \phi}{\partial z} = 0 \quad \text{at} \quad z = \pm 1/2 \tag{II.9}$$

$$\frac{\partial \phi}{\partial y} - \sigma_0^2 \phi = f_2(x,z) \tag{II.10}$$

The set (II.6) - (II.10) without the forcing terms is self adjoint. Define a function ψ which satisfies (II.6) - (II.10) with $f_1 = f_2 = 0$, then multiplying (A.6) by ψ, integrating over the domain, and using Green's theorem, results in the necessary condition for solvability

$$\int_{-1/2}^{1/2} \int_{-\infty}^{0} \int_{-1/2}^{1/2} \psi(x,y,z) f_1(x,y,z) dxdydz = \int_{-1/2}^{1/2} \int_{-1/2}^{1/2} \psi(x,0,z) f_2(x,z) dxdz \tag{II.11}$$

Appendix III

In this appendix the coefficients used in equations (3.7) and (3.8) for the analysis at double eigenvalues are defined,

$$A_{20} = \frac{-\sigma_0}{8} (A_{11}^2 + A_{12}^2)$$

$$A_{21} = \frac{\beta_n^2 A_{11}^2}{4\sigma_0(\alpha_m - 2\sigma_0^2)}$$

$$A_{22} = \frac{\beta_n^2 A_{12}^2}{4\sigma_0(\alpha_m - 2\sigma_0^2)}$$

$$A_{23} = \frac{\alpha_m^2 A_{12}^2}{4\sigma_0(\beta_n - 2\sigma_0^2)}$$

$$A_{24} = \frac{\alpha_m^2 A_{11}^2}{4\sigma_0(\beta_n - 2\sigma_0^2)}$$

$$A_{25} = \frac{A_{11} A_{12} (\alpha_m - \beta_n)^2}{2\sigma_0(\sqrt{2}(\alpha_m + \beta_n) - 4\sigma_0^2)}$$

$$A_{26} = \frac{A_{11}A_{12}\sigma_0}{2(\sqrt{2} - 4)}$$

$$A_{27} = \frac{A_{11}A_{12}(\alpha_m + \beta_n)^2}{2\sigma_0(\sqrt{2}|\alpha_m - \beta_n| - 4\sigma_0^2)}$$

$$B_{21} = \frac{\alpha_m^2 A_{11}^2}{8\sigma_0^2} \qquad C_{21} = -2\sigma_0 A_{21} - \frac{A_{11}^2}{8\sigma_0^2}(\sigma_0^4 + \beta_n^2)$$

$$B_{22} = \frac{\alpha_m^2 A_{12}^2}{8\sigma_0^2} \qquad C_{22} = -2\sigma_0 A_{22} - \frac{A_{12}^2}{8\sigma_0^2}(\sigma_0^4 + \beta_n^2)$$

$$B_{23} = \frac{\beta_n^2 A_{12}^2}{8\sigma_0^2} \qquad C_{23} = -2\sigma_0 A_{23} - \frac{A_{12}^2}{8\sigma_0^2}(\sigma_0^4 + \alpha_m^2)$$

$$B_{24} = \frac{\beta_n^2 A_{11}^2}{8\sigma_0^2} \qquad C_{24} = -2\sigma_0 A_{24} - \frac{A_{11}^2}{8\sigma_0^2}(\sigma_0^4 + \alpha_m^2)$$

$$B_{25} = \frac{A_{11}A_{12}}{8\sigma_0^2}(\alpha_m + \beta_n)^2 \qquad C_{25} = -2\sigma_0 A_{25} - \frac{A_{11}A_{12}}{8\sigma_0^2}(3\sigma_0^4 - 2\alpha_m\beta_n)$$

$$B_{26} = \frac{\sigma_0^2}{8} A_{11}A_{12} \qquad C_{26} = -2\sigma_0 A_{26} - \frac{3}{8}\sigma_0^2 A_{11}A_{12}$$

$$B_{27} = \frac{A_{11}A_{12}}{8\sigma_0^2}(\alpha_m - \beta_n)^2 \qquad C_{27} = -2\sigma_0 A_{27} - \frac{A_{11}A_{12}}{8\sigma_0^2}(3\sigma_0^4 + 2\alpha_m\beta_n)$$

$$B_{28} = A_{11}^2 \frac{\sigma_0^2}{8} \qquad C_{28} = -A_{11}^2 \frac{\sigma_0^2}{8}$$

$$B_{29} = A_{12}^2 \frac{\sigma_0^2}{8} \qquad C_{29} = -A_{12}^2 \frac{\sigma_0^2}{8}$$

Appendix IV

In this appendix the coefficients used in equations (4.25) and (4.26) for the analysis of the secondary bifurcation, are defined. They are not to be confused with those in Appendix III.

$$A_{00} = \frac{-\omega_0}{8}$$

$$A_{20} = \frac{-7}{32}\,\omega_0$$

$$A_{21} = \frac{-(\alpha_m^2 - 7\beta_n^2)}{16\omega_0(\alpha_m - 2\omega_0^2)}$$

$$A_{22} = \frac{-(\beta_n^2 - 7\alpha_m^2)}{16\omega_0(\beta_n - 2\omega_0^2)}$$

$$A_{23} = \frac{\omega_0}{16}$$

$$A_{24} = \frac{(3\omega_0^4 + 8\alpha_m\beta_n)}{8\omega_0(\sqrt{2}|\alpha_m - \beta_n| - 4\omega_0^2)}$$

$$A_{25} = \frac{(3\omega_0^4 - 8\alpha_m\beta_n)}{8\omega_0(\sqrt{2}(\alpha_m + \beta_n) - 4\omega_0^2)}$$

$$A_{26} = \frac{3\omega_0}{8(\sqrt{2} - 4)}$$

$$C_{20} = \frac{\omega_0^2}{16}$$

$$B_{21} = \frac{(\alpha_m^2 - \beta_n^2)}{8\omega_0^2} \qquad C_{21} = -2\omega_0 A_{21} - \frac{(\alpha_m^2 + 3\beta_n^2)}{8\omega_0^2}$$

$$B_{22} = \frac{(\beta_n^2 - \alpha_m^2)}{8\omega_0^2} \qquad C_{22} = -2\,\omega_0 A_{22} - \frac{(\beta_n^2 + 3\alpha_m^2)}{8\omega_0^2}$$

$$B_{23} = \frac{\omega_0^2}{8} \qquad C_{23} = -\frac{\omega_0^2}{4}$$

$$B_{24} = \frac{-\alpha_m\beta_n}{4\omega_0^2} \qquad C_{24} = -2\omega_0 A_{24} - \frac{(\omega_0^4 + \alpha_m\beta_n)}{4\omega_0^2}$$

$$B_{25} = \frac{\alpha_m\beta_n}{4\omega_0^2} \qquad C_{25} = -2\omega_0 A_{25} - \frac{(\omega_0^4 - \alpha_m\beta_n)}{4\omega_0^2}$$

$$C_{26} = \left(\frac{\sqrt{2} - 1}{4 - \sqrt{2}}\right)\frac{\omega_0^2}{4}$$

Appendix V

In this appendix the coefficients corresponding to the solutions along the secondary branches are given. They are used in equations (5.13), (5.14), (5.19), and (5.20).

$$A_{121} = \frac{-b_0(\alpha_m + \beta_n)^2}{2\omega_0[4\omega_0^2 - \sqrt{2}|\alpha_m - \beta_n|]}$$

$$A_{122} = \frac{-b_0(\alpha_m - \beta_n)^2}{2\omega_0[4\omega_0^2 - \sqrt{2}(\alpha_m + \beta_n)]}$$

$$A_{123} = \frac{-b_0\omega_0}{2(4 - \sqrt{2})}$$

$$B_{121} = \frac{b_0(\alpha_m - \beta_n)^2}{8\omega_0^2} \qquad C_{121} = -2\omega_0 A_{121} - \frac{3}{8}b_0\omega_0^2 - \frac{b_0\alpha_m\beta_n}{4\omega_0^2}$$

$$B_{122} = \frac{b_0(\alpha_m + \beta_n)^2}{8\omega_0^2} \qquad C_{122} = -2\omega_0 A_{122} - \frac{3}{8}b_0\omega_0^2 + \frac{b_0\alpha_m\beta_n}{4\omega_0^2}$$

$$B_{123} = \frac{b_0\omega_0^2}{8} \qquad C_{123} = -2\omega_0 A_{123} - \frac{3}{8}b_0\omega_0^2$$

$$A_{221} = \frac{\beta_n^2}{4\omega_0(2\omega_0^2 - \beta_n)}$$

$$A_{222} = \frac{\alpha_m^2}{4\omega_0(2\omega_0^2 - \alpha_m)}$$

$$A_{223} = \frac{\omega_0}{4}$$

$$B_{221} = \frac{\beta_n^2}{8\omega_0^2} \qquad C_{221} = -2\omega_0 A_{221} + \frac{\beta_n^2}{8\omega_0^2}$$

$$B_{222} = \frac{\alpha_m^2}{8\omega_0^2} \qquad C_{222} = -2\omega_0 A_{222} + \frac{\alpha_m^2}{8\omega_0^2}$$

$$B_{223} = \frac{\omega_0^2}{8} \qquad C_{223} = -3\frac{\omega_0^2}{8}$$

References

1. H. Lamb (1945) Hydrodynamics, Dover
2. G. H. Verma and J. B. Keller (1962) Three-Dimensional Standing Surface Waves of Finite Amplitude, Phys, Fluids, 5, 52-56
3. D. H. Sattinger (1983) Branching in the Presence of Symmetry, CBMF-NSF Conf. Notes, 40, SIAM
4. L. Bauer, H. B. Keller, and E. L. Reiss (1975) Multiple Eigenvalues Lead to Secondary Bifurcation, SIAM Review, 17, 101-122
5. T. J. Mahar and B. J. Matkowsky (1977) A Model Biochemical Reaction Exhibiting Secondary Bifurcation, SIAM J. Appl. Math., 32, 394-404
6. B. J. Matkowsky, L. J. Putnick, and E. L. Reiss (1980) Secondary States of Rectngular Plates, SIAM J. Appl. Math., 38, 38-51
7. E. L. Reiss (1983) Cascading Bifurcation, SIAM J. Appl. Math., 43, 57-65
8. G. I. Taylor (1953) An Experimental Study of Standing Waves, Proc. Roy. Soc.A 218, 44-59
9. *T. J. Bridges and P. J. Morris* (1984) Differential Eigenvalue Problems in Which the Parameter Appears Nonlinearly, J. Comp. Phys., 55, 437-460
10. L. W. Schwartz and A. K. Whitney (1981) A Semi-Analytic Solution for Nonlinear Standing Waves in Deep Water, J. Fluid Mech, 107, 147-171
11. L. S. Cheo and E. L. Reiss (1974) Secondary Buckling of Circular Plates, SIAM J. Applied Math, 26, 490-495
12. L. R. Mack (1962) Periodic, Finite Amplitude, Axisymmetric Gravity Waves, J. Geophys. Res, 67, 829-843

TJB/jp

SECURITY CLASSIFICATION OF THIS PAGE *(When Data Entered)*

REPORT DOCUMENTATION PAGE		READ INSTRUCTIONS BEFORE COMPLETING FORM
1. REPORT NUMBER #2839	2. GOVT ACCESSION NO. AD-A160 971	3. RECIPIENT'S CATALOG NUMBER
4. TITLE *(and Subtitle)* ON THE SECONDARY BIFURCATION OF THREE DIMENSIONAL STANDING WAVES		5. TYPE OF REPORT & PERIOD COVERED Summary Report - no specific reporting period 6. PERFORMING ORG. REPORT NUMBER
7. AUTHOR(s) Thomas J. Bridges		8. CONTRACT OR GRANT NUMBER(s) DAAG29-80-C-0041 DMS-8210950, Mod. 1.
9. PERFORMING ORGANIZATION NAME AND ADDRESS Mathematics Research Center, University of Wisconsin 610 Walnut Street Madison, Wisconsin 53706		10. PROGRAM ELEMENT, PROJECT, TASK AREA & WORK UNIT NUMBERS Work Unit Number 2 - Physical Mathematics
11. CONTROLLING OFFICE NAME AND ADDRESS See Item 18 below		12. REPORT DATE July 1985 13. NUMBER OF PAGES 51
14. MONITORING AGENCY NAME & ADDRESS*(if different from Controlling Office)*		15. SECURITY CLASS. *(of this report)* UNCLASSIFIED 15a. DECLASSIFICATION/DOWNGRADING SCHEDULE

16. DISTRIBUTION STATEMENT *(of this Report)*

Approved for public release; distribution unlimited.

17. DISTRIBUTION STATEMENT *(of the abstract entered in Block 20, if different from Report)*

18. SUPPLEMENTARY NOTES

U. S. Army Research Office
P. O. Box 12211
Research Triangle Park
North Carolina 27709

National Science Foundation
Washington, D. C. 20550

19. KEY WORDS *(Continue on reverse side if necessary and identify by block number)*

Three-Dimensional Non-Linear Standing Waves, Multiple eigenvalues, secondary bifurcation

20. ABSTRACT *(Continue on reverse side if necessary and identify by block number)*

This paper contains an analysis of the complex set of periodic solutions which may occur in a fluid filled vessel of rectangular cross section. A previous analysis by Verma and Keller [2] found only simple eigenvalues for the linearized problem. It is shown herein that at critical values of the vessel aspect ratio double eigenvalues occur. Eight non-linear solution branches are emitted from these double eigenvalues. The solutions along the various branches are derived, and the results displayed graphically. It is shown that irregular waves occur along some of these branches.

DD FORM 1 JAN 73 1473 EDITION OF 1 NOV 65 IS OBSOLETE

UNCLASSIFIED

SECURITY CLASSIFICATION OF THIS PAGE *(When Data Entered)*

20. In an interesting development, Bauer, Keller, and Reiss [4], in their analysis of shell buckling, showed that the splitting of multiple eigenvalues may lead to secondary bifurcation. This theory is applied to the non-linear standing wave problem herein, and it is shown that secondary bifurcation does occur in the neighborhood of the double eigenvalue. A perturbation method is used to find the secondary bifurcation points, and the solutions along the secondary branches, in the neighborhood of their respective branch points, are found.

The neighborhood around the critical aspect ratios is substantial, suggesting that secondary branching may occur in a variety of vessels with rectangular cross section. This theory offers an explanation of the irregular waves often observed in the "sloshing" of fluid in a rectangular vessel.

END

FILMED

12-85

DTIC